The Use of a Base Isolation System for an Emergency Diesel Generator to Reduce the Core Damage Frequency Caused by a Seismic Event

Young-Sun Choun[1)], Min-Kyu Kim[1)] and Yasuki Ohtori[2)]

1) Integrated Risk Assessment Center, Korea Atomic Energy Research Institute, Daejeon, Korea
2) Earthquake Engineering Sector, Central Research Institute of Electric Power Industry, Abiko, Japan

ABSTRACT

A seismic-induced core damage frequency (CDF) of a nuclear power plant can be remarkably reduced by an application of a base isolation system for an Emergency Diesel Generator (EDG). The effectiveness of the seismic isolation effect of a base isolation system for an EDG set was demonstrated through a shaking table test for a scaled EDG model by using a uniform hazard spectrum. The results of the shaking table test demonstrated that the base isolation system can significantly reduce the seismic force transmitted to an EDG set from the table. A seismic fragility analysis method for a base isolated structure was developed, and then the effect of a seismic isolation of an EDG set on its seismic fragility curve was investigated through a fragility analysis. It is shown that the probability of a failure of the EDG set is dramatically decreased by introducing the base isolation system, and, as a result, the HCLPF (High Confidence of Low Probability of Failure) value increases remarkably. Finally, when the base isolation system is introduced to the EDG set, the core damage frequencies were evaluated. A case study showed that a reduction of 47 percent of a seismic-induced CDF can be achieved by the base isolation system, and finally a plant level CDF can be reduced by 19 percent.

INTRODUCTION

An Emergency Diesel Generator (EDG) is the primary power source to supply AC power to the Class 1E power systems and equipment when the main turbine generator and offsite power source are not available in nuclear power stations. The EDG reduces the probability of a station blackout (SBO) due to a failure of AC power and finally it reduces the core damage frequency. For the purpose of improving the integrity of an EDG set, a spring-damper system has been adopted as a vibration and seismic isolation system because it is able to reduce the mechanical vibration level on the floor during an operation of the engine as well as the seismic force transmitted to an EDG body from the ground during an earthquake[1-3].

The basic concept of a base isolation is to decouple a structure from the horizontal components of an earthquake ground motion by interposing a soft layer with a low horizontal stiffness between the structure and the foundation. This soft layer gives the structure a much lower fundamental frequency than its fundamental frequency for a fixed base and also much lower than the predominant frequencies of the ground motion. When a destructive earthquake occurs, since most of the deformation behavior is concentrated on the soft layer, the remainder of the structure will remain nearly elastic. Thus, a floor acceleration and interstory drift of a structure will be significantly reduced and also damage to structural elements will be dramatically reduced. Also, the elastic behavior of an isolated structure will give a more reliable response than conventional structures. An application of a base isolation system to nuclear facilities will improve the plant safety margin against the design basis earthquake as well as a beyond design basis seismic event due to its superior seismic performance. Base isolation of individual components is especially beneficial in a situation where existing components and their supports have to be requalified for higher seismic loads. By using a base isolation, it may be possible to avoid an expensive retrofitting of a supporting facility and foundation.

There are limited studies on a seismic isolation of equipment and components in spite of the potential advantages that an application of a base isolation system for equipment and components can improve the seismic safety of a nuclear power plant. Kelly[4], Hall[5], and Ebisawa et al.[6] proposed the use of base isolation systems for improving the seismic capacity of various components. The results of their studies indicate that the use of a base isolation in light secondary equipment or a large component can be beneficial in reducing the accelerations experienced by a component. Especially, Ebisawa et al. studied a base isolation of a nuclear component by experimental and numerical methods, and developed the technical basis for a seismic isolation of nuclear components. They also carried out various experiments including field tests against real earthquakes in order to obtain test data for a component base isolation. They concluded in their study that a seismic base isolation can improve the seismic resistance of nuclear components and decrease their functional failure probability. Huang et al.[7] showed that considerable reductions of the seismic demands on secondary systems in a nuclear power plant can be realized by seismic isolation systems. Also, recent studies have shown that the increase of a seismic capacity of an Emergency Diesel Generator can remarkably reduce the core damage frequency in nuclear power plants[8, 9].

This study evaluates a core damage frequency (CDF) of a nuclear power plant when an Emergency Diesel Generator is mounted on a base isolation system. Firstly, the contribution of a failure of equipment and components to the CDF was investigated and a failure mode of each equipment and component was also investigated. Secondly, the seismic isolation effect of the base isolation system for the EDG set was evaluated through a shaking table test for a scaled EDG model by using a uniform hazard spectrum. Thirdly, a seismic fragility analysis method for a base isolated structure was developed, and then the effect of a seismic isolation of an EDG set on its seismic fragility curve was

investigated through a fragility analysis. Finally, when the base isolation system is introduced to the EDG set, the core damage frequencies were evaluated through a case study.

CONTRIBUTION TO CORE DAMAGE FREQUENCY

The contribution of a seismic-induced failure of a component or equipment to the plant core damage frequency was evaluated for most nuclear power plants in Korea. Figure 1 shows the contribution ratios of safety-related components and equipment to the seismic-induced CDF for Yonggwang Nuclear Unit 5&6, Ulchin Nuclear Unit 3&4, and Ulchin Nuclear Unit 5&6. It is found from Figure 1 that an Emergency Diesel Generator, an Offsite Power System, a Condensate Storage Tank, a Battery Rack, and a Battery Charger have a high contribution to the seismic-induced CDF in nuclear power plants. Above all, the contribution ratio of the EDG is so high that an increase of the seismic capacity of an EDG is essential to reduce the total plant CDF. The CDF contribution ratios of the EDG in Yonggwang Nuclear Unit 5&6, Ulchin Nuclear Unit 3&4, and Ulchin Nuclear Unit 5&6 are 29.8, 20.5, and 29.7 percent, respectively.

Table 1 shows a failure mode and a HCLPF (High Confidence of Low Probability of Failure) value of the important equipments for each nuclear unit. The HCLPF value of the EDG is relatively lower than that of the Condensate Storage Tank. Therefore, if one equipment item or component has to be selected for improving the seismic safety of a nuclear power plant, the first choice should be the EDG. The failure mode of the EDG is known as a concrete coning failure due to a pulling out of the anchor bolts as shown in Table 1. Thus, to increase the seismic capacity of the EDG, a base isolation system can be introduced instead of an anchor bolt.

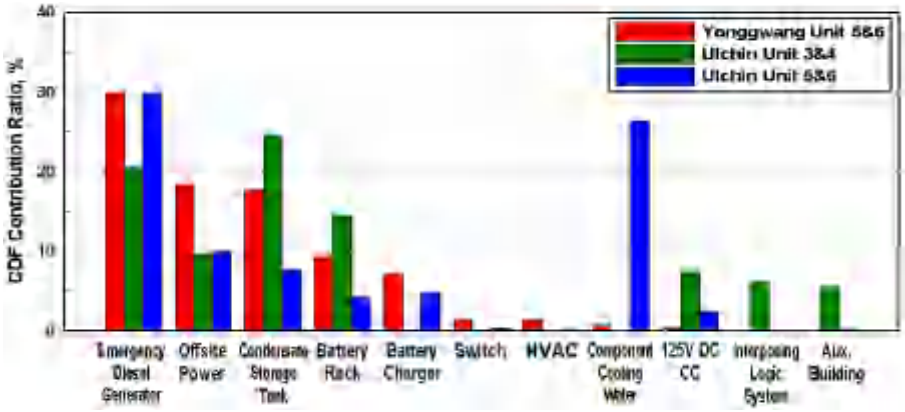

Fig. 1 CDF contribution ratios of the major equipment and components at Korean NPPs[10]

Table 1. Failure mode and HCLPF value

Nuclear Unit	Equipment/Components	Failure Mode	HCLPF (g)
Yonggwang Unit 5&6	Diesel Generator	Concrete Coning	0.38
	Offsite Power	Functional Failure	0.15
	Condensate Storage Tank	Structural Failure	0.41
	Battery Rack	Structural Failure	0.72
	Battery Charger	Functional Failure	0.41
		Structural Failure	0.52
Ulchin Unit 3&4	Diesel Generator	Concrete Coning	0.38
	Offsite Power	Functional Failure	0.15
	Condensate Storage Tank	Structural Failure	0.41
	Battery Rack	Structural Failure	0.43
Ulchin Unit 5&6	Diesel Generator	Concrete Coning	0.38
	Offsite Power	Functional Failure	0.15
	Condensate Storage Tank	Structural Failure	0.45
	ESW Pump	Anchorage	0.47
	CCW Surge Tank	Concrete Coning	0.47

EFFECTIVENESS OF A SEISMIC ISOLATION

For a base isolation of rotating equipment such as an EDG, especially, a coil spring-viscous damper system is suitable because a mechanical vibration in a vertical direction is generated during an operation and it is reduced by a coil spring with a low vertical stiffness[11]. Thus, a coil spring-viscous damper system has been adapted to vibrating machines to reduce their mechanical vibration during an operation as well as their seismic force during an earthquake. This study evaluates the seismic effectiveness of a coil spring-viscous damper system through a seismic test of a scaled model of a base-isolated EDG on a shaking table. As a prototype, an EDG set with a HANJUNG-SEMT Pielstick Engine 16PC2-5V 400 was chosen, which is identical to the EDG installed at Yonggwang Nuclear Unit 5&6, Wolsung 2, 3&4 and Ulchin Nuclear Unit 3&4, 5&6 of Korea, and the scaled model was designed to represent the seismic behavior of a prototype of an EDG set. The dynamic characteristics of the coil spring-viscous damper system were obtained by cyclic tests and the seismic responses of the base-isolated EDG model were obtained by shaking table tests.

EDG Test Model

The prototype of the EDG set consists of an engine unit, a generator unit, and a concrete mass. Net weights of the engine unit, the generator unit, and the concrete mass are 912 kN, 392 kN, and 2,474 kN, respectively, and the total weight is 3,779 kN. A 6-DOF seismic simulator with a table dimension of 2.5 m × 2.5 m was used for the model test. Test model was designed by considering the size of the shaking table of the simulator as shown in Figure 2, which consists of a concrete block of 2,300 mm × 800 mm × 450 mm, four steel blocks of 600 mm × 600 mm × 140 mm, and two steel plates of 1,500 mm × 300 mm × 30 mm. Total weight of the test model is 39 kN and the steel blocks were placed to have an equivalent mass center of the prototype.

For the seismic isolation of the EDG test model, a coil spring-viscous damper unit that consists of a combination of 2 coil springs and one viscous damper was adapted. The stiffnesses and the damping coefficients of the coil spring-viscous damper unit for the vertical and horizontal directions were determined by the seismic responses of the EDG test model for the input motion. The test model was supported by 4 coil spring-viscous damper units as shown in Figure 2.

Item		Properties
Load Capacity		15 kN
Height		410 mm
Stiffness	Vertical	0.144 kN/mm
	Horizontal	0.04 kN/mm
Damping Coefficient	Vertical	3.5 kNs/m
	Horizontal	4.0 kNs/m

Fig. 2 EDG model with spring-damper units for the shaking table test

Shaking Table Test

An artificial time-history corresponding to the uniform hazard spectrum[12] was used and three peak acceleration levels of 0.1g, 0.2g, and 0.3g were applied for the input table motion. Seismic tests were carried out for one and three directional excitations. Identical input motions and peak acceleration levels were used in two horizontal directions and one vertical direction. Figure 3 shows the artificial time history and response spectrum of the input motion. The acceleration and displacement responses were measured by using two accelerometers and eight LVDTs.

Test Results

Figure 4 shows the spectral accelerations for the peak acceleration level of 0.2g during one and three directional excitations together with the table motions. It is found that the spectral accelerations decrease significantly due to a shift

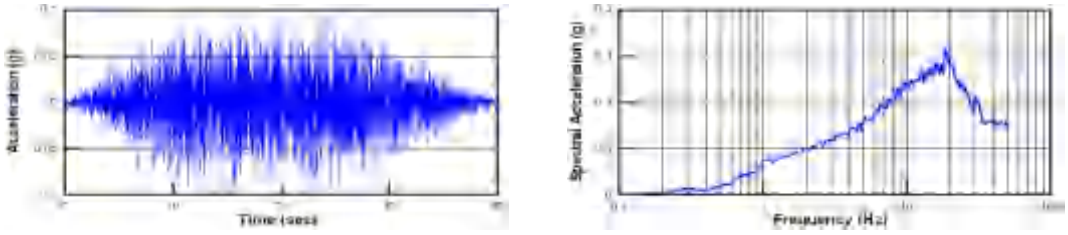

(a) Artificial time-history (b) Response spectrum

Fig. 3 Input motion for the shaking table tests

of the predominant frequency from 20Hz to 1.0Hz, and the differences between the acceleration responses in the one horizontal excitation and the three directional excitations are very small. Figure 5 shows the horizontal and vertical acceleration response ratios, which are determined as a ratio of the peak acceleration response for the test model to the peak acceleration of the shaking table, for different acceleration levels and excitation directions. There was a small difference in the acceleration response ratios between the two accelerometers (A1, A2) because the mass center was not located at the center of the test model. The average response ratios for the horizontal and vertical directions are 0.5 and 0.7, respectively. This indicates that the coil spring-viscous damper system can reduce the seismic force transmitted to the EDG model from the table by up to 50 percent in the horizontal direction and 30 percent in the vertical direction, respectively. This result demonstrates that the seismic capacity of an EDG set can be effectively improved by using a base isolation system. The acceleration response ratios can be minimized by an optimum design of the base isolation system.

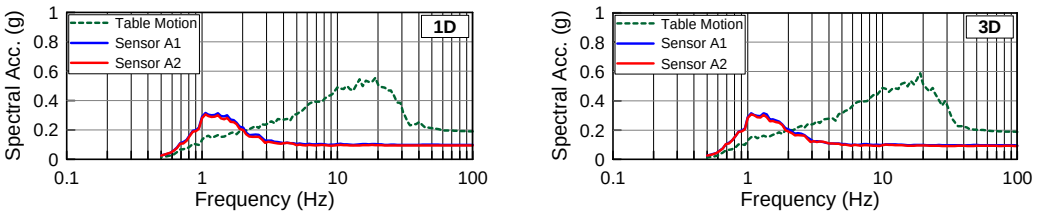

(a) One horizontal excitation (b) Three directional excitations

Fig. 4 Spectral accelerations for the peak acceleration of 0.2g

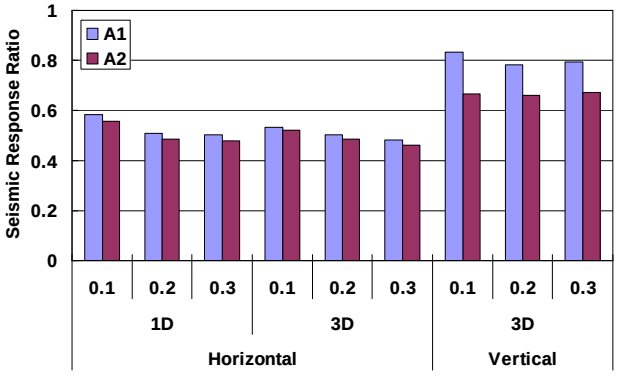

Fig. 5 Comparisons of acceleration response ratios for the isolated EDG model

FRAGILITY ANALYSIS

It is known that the major failure mode of an EDG is a concrete coning failure due to a pulling out of the anchor bolts as shown in Table 1. However, if applying the base isolation system to the EDG, the major failure mode will not be a concrete coning failure any more. The governing failure mode of the base-isolated EDG must be a failure of the isolation system. Thus, the fragility curves for a base-isolated EDG should be different from those for a conventional type. This study developed a fragility analysis method for a base-isolated structure and investigated the effect of a seismic isolation of an EDG set on its seismic fragility curve.

Fragility Analysis Method

A simple fragility analysis method which uses only one seismic input motion was proposed[13]. The proposed method uses a relation regarding the seismic response and input seismic motion. The probability of a structural failure regarding an input seismic motion is defined by Eq. (1).

$$F_A(A) = \int_0^{\infty} f_R(A, x_R) \int_0^{x_R} f_C(x)dx \; dx_R \tag{1}$$

where, f_R is a probability density function of a seismic response, and f_C is that of the capacity. Equation (1) can also be represented as Eq. (2).

$$F_A(A) = 1 - \Phi\left[\frac{\ln C_m - \ln R_m(A)}{\sqrt{\beta_C^2 + \beta_R(A)^2}}\right] \tag{2}$$

where, β_C and β_R are an uncertainty of capacity and response, respectively. A relation of the mean response and the median response can be given as in Eq. (3).

$$R_m(A) = \frac{\overline{R(A)}}{\sqrt{1 + \frac{\sigma_R}{\overline{R(A)}}}} = \overline{R(A)} \cdot e^{-\frac{1}{2}\beta_R^2} \tag{3}$$

Using Eq. (3), Eq. (2) can be rewritten as Eq. (4).

$$F_A(A) = 1 - \Phi\left[\frac{\ln C_m - \ln\overline{R(A)} - \frac{1}{2}\beta_R^2(A)}{\sqrt{\beta_C^2 + \beta_R(A)^2}}\right] \tag{4}$$

where, $\ln\overline{R(A)}$ is a logarithm of the mean response. The relation of $F_A(A)$ and A represents the probability of a failure.

Fragility Analysis

A fragility analysis was carried out for a base-isolation and non-isolation EDG set. Since the natural frequency of the EDG set is about 34Hz, its dynamic behavior is similar to a rigid body motion. Thus, a numerical model of a single degree of freedom system as shown in Figure 6 was used for the fragility analysis. The weight of the EDG is modeled as a lumped mass at the mid-height and spring elements which consist of two springs for the horizontal direction and one spring for the vertical direction are introduced at the base of the EDG in order to represent the behavior of the base isolation system. The identical input seismic motion used for the shaking table test was applied for the fragility analysis. The failure criterion for the fragility analyses were assumed as a maximum acceleration response of 1.2g and a maximum displacement limit of 5cm.

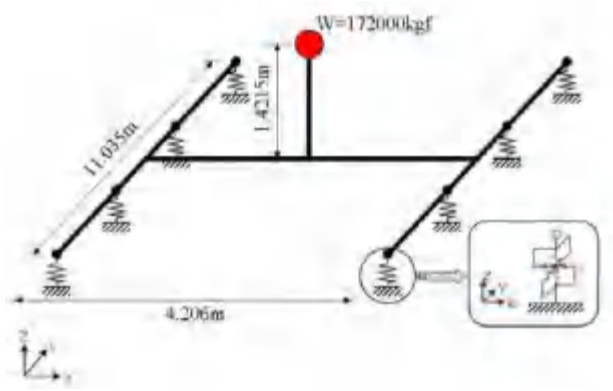

Fig. 6 Numerical model of a base-isolated EDG

The results of the fragility analysis for various damping coefficients are shown in Figure 7. The figure shows that when an EDG is supported by a base isolation system, the failure probability of the EDG body will be significantly decreased because the governing failure mode of an isolated EDG will be the failure of an isolator. The fragility curves are very sensitive to the damping value of an isolation system. For a larger damping value, the probability of a failure will be low. The HCLPF values of the base-isolated EDG set determined with the same parameters are shown in Figure 8. It is found that the failure of an isolator governs the probability of a failure of the isolated EDG set except with a damping ratio of over 10 percent and the probability of a failure of the isolated EDG set is dramatically decreased. As a result it can be said that the seismic safety of an EDG set is increased by using a base isolation system.

The fragility curves of the base-isolated EDG set for various failure criteria of the displacement of an isolator are shown in Figure 9. It is easily seen that the probability of a failure will be low for the limitation of a large displacement. The HCLPF values for various failure criteria of the displacement of an isolator are shown in Table 2. The HCLPF value

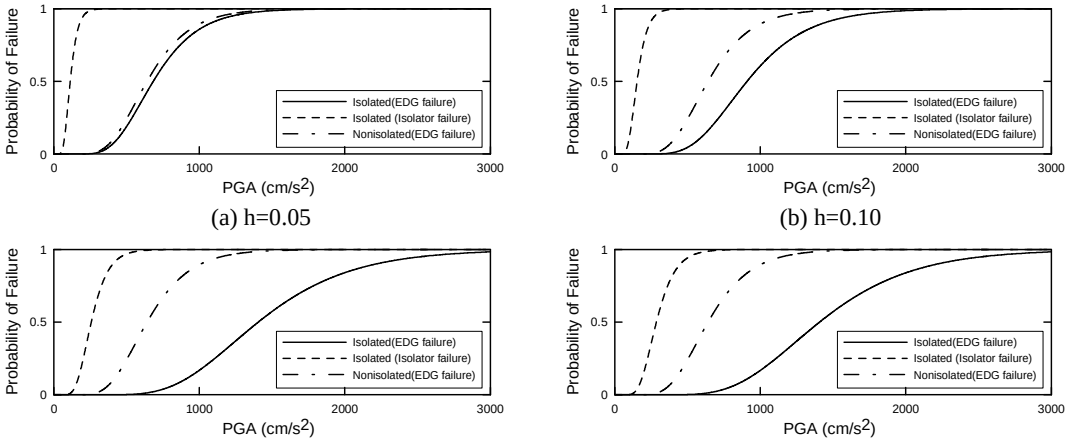

(a) h=0.05 (b) h=0.10

(c) h=0.25 (d) h=0.40

Fig. 7 Fragility curves of the isolated EDG set for different damping ratios

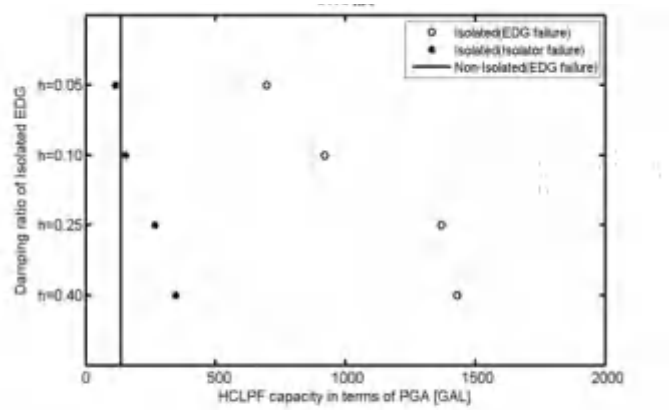

Fig. 8 HCLPF values of the isolated EDG set for different damping ratios

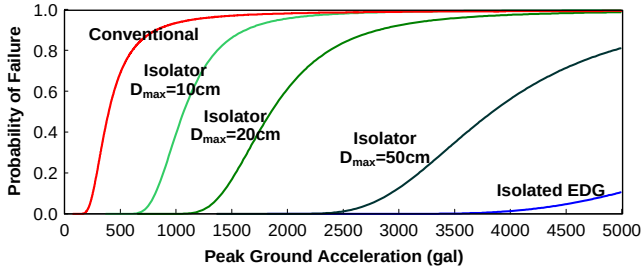

Fig. 9 Fragility curves of the isolated EDG set for displacement failure criteria

Table 2. HCLPF values for the displacement failure criteria

Type	HCLPF (gal)
Conventional EDG	192
Isolated, D_{max}=10 cm	687
Isolated, D_{max}=20 cm	1,192
Isolated, D_{max}=50 cm	2,470
Isolated, no failure at isolators	3,903

is very sensitive to the displacement failure criteria of an isolator, and the HCLPF value is significantly increased with an increase of an allowable displacement of an isolator. For instance, when the maximum displacement of the isolator is limited to 10 cm, the HCLPF value increases by 3.6 times the HCLPF value for a conventional EDG, and when the maximum displacement of the isolator is limited to 20 cm, the HCLPF value increases by 6.2 times the HCLPF value for a conventional EDG.

CORE DAMAGE FREQUENCY

Core damage frequencies were evaluated through a case study for Yonggwang Unit 5&6 when a base isolation system is introduced to an EDG set only. In general, a seismic-induced CDF is reduced with an increase of the seismic capacity of an EDG. However, there is a limitation in the reduction of the seismic-induced CDF. For a larger HCLPF value than an effective value, even though the seismic capacity increases, the seismic-induced CDF does not decrease any more as shown in Figure 10. For the EDG, it is found from Figure 10 that there is little decrease in the seismic-induced CDF for a HCLPF value greater than 0.84g.

A seismic-induced CDF and a total CDF for Yonggwang Unit 5&6 were originally calculated as 7.79E-06 and 1.76E-05, respectively. When the HCLPF value of the EDG reaches 0.84g by introducing a base isolation system, a seismic-induced CDF and a total CDF were calculated as 4.46E-06 and 1.42E-05 as shown in Table 3, respectively. This indicates that a reduction of 47 percent in a seismic-induced CDF can be achieved by the base isolation system, and finally a total CDF can be reduced by 19 percent.

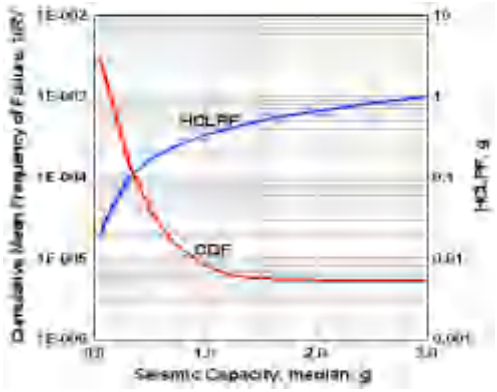

Fig. 10 Relations between the HCLPF of an EDG and the CDF[9]

Table 3. Comparison of the CDF between the non-isolated and isolated cases

Event	Non-Isolation	Base Isolation
Internal	7.43E-06	7.43E-06
Seismic	7.79E-06	4.46E-06
Fire	2.35E-06	2.35E-06
Total	1.76E-05	1.42E-05

CONCLUSION

This study evaluates a CDF of a nuclear power plant when a base isolation system is introduced to an EDG set. An EDG set reveals a high contribution to a seismic-induced CDF but its HCLPF value is not high. Thus, if one equipment item or component has to be selected for improving the seismic safety of a nuclear power plant, the first choice should be the EDG. Since the failure mode of the EDG is known as a concrete coning failure due to a pulling out of the anchor bolts, the use of a base isolation system instead of an anchor bolt will increase the seismic capacity of an EDG.

A base isolation system is very effective for an improvement of the seismic capacity of equipment or components. The effectiveness of the seismic isolation effect of a base isolation system for an EDG set was demonstrated through a shaking table test for a scaled EDG model by using a uniform hazard spectrum. The coil spring-viscous damper system for the EDG could reduce the seismic force transmitted to the EDG model from the table by up to 50 percent in the horizontal direction and 30 percent in the vertical direction, respectively. The seismic capacity of an EDG set can be effectively improved by using a base isolation system.

The seismic fragility curves for a base-isolated EDG will be different from those for a conventional type. The results of seismic fragility analyses by using a simple method proposed in this study showed that the fragility curves were very sensitive to the damping value of an isolation system and the HCLPF value was very sensitive to the displacement failure criteria of an isolation system. The probability of a failure will be low for a larger damping value and the HCLPF value is significantly increased with an increase of an allowable displacement of an isolation system. An introduction of a base isolation system to an EDG set will reduce its failure probability and increase its HCLPF value.

In general, a seismic-induced CDF is reduced with an increase of the seismic capacity of an EDG. However, for a larger HCLPF value than an effective value, even though the seismic capacity increases, the seismic-induced CDF does not decrease any more. The effective HCLPF value for the EDG in Yonggwang Unit 5&6 was determined as 0.84g. There is little decrease in the seismic-induced CDF for a HCLPF value of an EDG greater than 0.84g for Yonggwang Unit 5&6. When the HCLPF value of the EDG reaches 0.84g by introducing a base isolation system, a reduction of 47 percent in a seismic-induced CDF can be achieved, and finally a total CDF can be reduced by 19 percent.

A base isolation is a very powerful concept to improve the seismic safety of nuclear power plants through its introduction to their safety-related structures and components. A seismic-induced CDF and a total CDF could be significantly reduced by introducing a base isolation system to the facilities which reveal a high contribution to a seismic-induced CDF. A base isolation concept can be effectively applied to all nuclear facilities including buildings, liquid storage tanks, turbine and diesel generators, transformers, mechanical and electrical equipment, and secondary systems. Base isolation of individual components is especially beneficial in a situation where existing components and their supports have to be requalified for higher seismic loads. By using a base isolation, it may be possible to avoid an expensive retrofitting of a supporting facility and foundation.

ACKNOWLEDGEMENT

This research was supported by the Mid- and Long-Term Nuclear Research & Development Program of the Ministry of Science and Technology, Korea.

REFERENCES

1. Huffmann, G.K., “Full Base Isolation for Earthquake Protection by Helical Springs and Viscodampers,” Nuclear Engineering and Design, Vol. 84, 1985, pp. 331-338.
2. GERB Schwingungsisolierungen GmbH & Co. KG, Vibration Isolation Systems, 10th Edition, Berlin, Germany, 2000.
3. Kostarev, V.V., Petrenko, A.V. and Vasilyev, P.S., “An Advanced Seismic Analysis of NPP Powerful Turbogenerator on Isolation Pedestal,” Transactions of the 18th International Conference on Structural Mechanics in Reactor Technology, paper A01/5, Beijing, China, August 7-12, 2005.
4. Kelly, J.M., The Influence of Base Isolation on the Seismic Response of Light Secondary Equipment, UCB/EERC-81/17, Earthquake Engineering Research Center, University of California, Berkeley, California, 1982.
5. Hall, D., The Use of Base Isolation and Energy-Absorbing Restrainers for the Seismic Protection of a Large Power Plant Component, EPRI NP-2918, Electric Power Research Institute, Palo Alto, California, 1983.
6. Ebisawa, K., Ando, K. and Shibata, K., “Progress of a Research Program on Seismic Base Isolation of Nuclear Components,” Nuclear Engineering and Design, Vol. 198, 2000, pp. 61-74.
7. Huang, Y.N., Whittaker, A.S., Constantinou, M.C. and Malushte, S., “Seismic Protection of Secondary Systems in Nuclear Power Plant Facilities,” Transactions of the 18th International Conference on Structural Mechanics in Reactor Technology, paper K11/7, Beijing, China, August 7-12, 2005.
8. Choun, Y.S., Choi, I.K. and Seo, J.M., “Improvement of Seismic Safety of Nuclear Power Plants by Increase of Equipment Seismic Capacity,” Proceedings of the 13th World Conference on Earthquake Engineering, paper No. 1915, Vancouver, Canada, August 1-6, 2004.
9. Choun, Y. S. and Choi, I. K., “Effect of the Seismic Capacity of Equipment on the Core Damage Frequency in Nuclear Power Plants,” Transactions of the 18th International Conference on Structural Mechanics in Reactor Technology, paper M01/3, Beijing, China, August 7-12, 2005.
10. Korea Electric Power Coporation, Ulchin Unit 3&4 Final Probabilistic Safety Assessment Report, 1992.
11. Choun, Y.S., Kim, M.K. and Seo, J.M., “Seismic and Vibration Isolation of an Emergency Diesel Generator by Using a Spring-Viscous Damper System,” Transactions of the 19th International Conference on Structural Mechanics in Reactor Technology, Toronto, Canada, August 12-17, 2007.
12. Choi, I.K., Choun, Y.S. and Seo, J.M., “Development of a Uniform Hazard Spectrum for a Soil Site by Considering the Site Soil Condition,” Transactions of the Korean Nuclear Society Spring Meeting, Gyeongju, Korea, May 27-28, 2004.
13. Choun, Y.S., Ohtori, Y., Choi, I.K., Kim, M.K., Shiba, Y. and Nakajima, M., Korea-Japan Joint Research on Development of Seismic Capacity Evaluation and Enhancement Technology Considering Near-Fault Effect, KAERI/RR-2688/2006, Korea Atomic Energy Research Institute, December 2006.

Seismic and Vibration Isolation of an Emergency Diesel Generator by Using a Spring-Viscous Damper System

Young-Sun Choun, Min-Kyu Kim and Jeong-Moon Seo

Integrated Risk Assessment Center, Korea Atomic Energy Research Institute, Daejeon, Korea

ABSTRACT

The effectiveness of a coil spring-viscous damper system for a vibration and seismic isolation of an Emergency Diesel Generator (EDG) was evaluated through a measurement of its operational vibration and seismic responses. The vibration measurement for an identical EDG set with different base systems - one with an anchor bolt system and the other with a coil spring-viscous damper system - was conducted during an operation to investigate the performance of a vibration isolation. The measurement showed that the vibration on the steel frame which supports the EDG set is significantly amplified but the vibration amplitude on the floor slab is negligible because much of the vibration on the steel frame is thoroughly isolated by the spring-damper system. A shaking table test for an EDG model was conducted for an evaluation of the seismic isolation performance of a coil spring-viscous damper system. An artificial time-history corresponding to the scenario earthquake for a Korean nuclear site was used as an input motion, and three peak acceleration levels were applied. The effectiveness of the coil spring-viscous damper system was evaluated by the ratio of the maximum acceleration responses measured at the model to the table acceleration. The vibration measurement during an operation of the EDG demonstrated that the spring-viscous damper system could reduce its mechanical vibration by more than 80 percent. Also, the EDG model tests showed that the spring-viscous damper system could reduce the seismic force transmitted to the EDG by up to 70 percent.

INTRODUCTION

Base isolation is a well-known and considerably mature technology to protect structures from strong earthquakes. A number of base isolation systems have been developed all over the world since 1970s. Some of them, for example rubber bearings and friction systems, have been adopted widely for buildings and civil structures such as bridges in several countries of a high seismicity, and their effectiveness has been demonstrated through surviving real strong earthquakes. The basic concept of a base isolation is to decouple a structure from the horizontal components of an earthquake ground motion by interposing a soft layer with a low horizontal stiffness between the structure and the foundation. This soft layer gives the structure a much lower fundamental frequency than its fundamental frequency for a fixed base and also much lower than the predominant frequencies of the ground motion. When a destructive earthquake occurs, since most of the deformation behavior is concentrated on the soft layer, the remainder of the structure will remain nearly elastic. Thus, a floor acceleration and interstory drift of the structure will be significantly reduced and also damage to the structural elements will be dramatically reduced. Also, the elastic behavior of the isolated structure will give a more reliable response than conventional structures.

In spite of the many potential advantages of a base isolation, however, the applications of a base isolation to nuclear facilities have been very limited because of a lack of sufficient data for the long-term operation of isolation devices. Since 1984, six large pressurized water reactor units have been isolated in France and South Africa[1,2]. At the Cruas plant in France, where the site safe shutdown earthquake (SSE) acceleration was 0.2g, four units were constructed on base isolation devices. Each of the four units is supported on 1,800 neoprene pads. At the Koeberg nuclear power station in South Africa, where the site SSE acceleration was 0.3g, two units were isolated. A total of 2,000 neoprene pads with friction plates were used.

The most important advantage of base isolation applications in nuclear power plants is that the safety and reliability of the plants can be remarkably improved through a standardization of the structures and equipment regardless of the seismic conditions of the sites. The standardization of structures and equipment will reduce the capital cost and design/construction schedule for future plants. Also, a base isolation can facilitate in a decoupling of the design and development for equipment, piping, and components due to the use of the generic in-structure response spectra associated with a standardized plant. Moreover, a base isolation will improve the plant safety margin against the design basis earthquake as well as a beyond design basis seismic event due to its superior seismic performance. Base isolation of individual components is especially beneficial in a situation where existing components and their supports have to be requalified for higher seismic loads. By using a base isolation, it may be possible to avoid an expensive retrofitting of the supporting facility and foundation.

Recent studies have shown that the use of base isolation devices instead of anchor bolts for an Emergency Diesel Generator (EDG) can remarkably increase the seismic resistance of the EDG and finally reduce the core damage frequency in a nuclear power plant[3,4]. For a base isolation of rotating equipment such as an EDG, specially, a coil spring-viscous damper system is suitable because a mechanical vibration in a vertical direction is generated during an operation and it is reduced by a coil spring with a low vertical stiffness. Thus, a coil spring-viscous damper system has been adapted to vibrating machines to reduce their mechanical vibration during an operation as well as the seismic force during an earthquake[5-7]. This study demonstrates the effectiveness of a coil spring-viscous damper system for a vibration and seismic isolation of EDG sets through a measurement of their operational vibration and seismic responses.

SPRING-VISCOUS DAMPER SYSTEM

A helical spring-viscous damper system is a well-known isolation device to effectively reduce structural and mechanical vibrations as well as seismic response in highly seismic areas. The system is suitable for a vibration isolation of structures especially against the vertical motions of mechanical vibrations or earthquakes. The helical springs support the weight of the structure and allow its motion in all three directions by their low horizontal and vertical stiffnesses. Steel helical springs are very adequate for a vibration isolation since the ratio between their vertical and horizontal stiffnesses is able to be easily varied to meet the required system frequency. Viscous dampers minimize undesirable motions in all possible directions by absorbing earthquake energy. The viscous dampers can provide a sufficient amount of damping, up to 20-30 percent of a critical damping, in all three directions and reduce the response of the structure considerably. Especially, a damping is desirable when passing resonance zones of a system during a start-up and shutdown of rotating equipment.

Viscous dampers consisting of a moving piston immersed in a highly viscous fluid show a behavior that is both elastic and viscous. The piston may move in all directions within the damper housing, thus providing a three-dimensional damping. Their mechanical properties are strongly frequency dependent, i.e., high damping in the lower frequency range of system resonances and earthquake motions but a negligible damping only in the operational speed range of the equipment as shown in Figure 1.

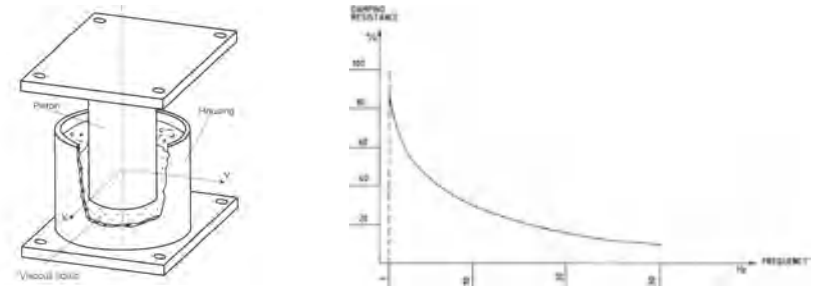

Fig. 1 Typical viscous damper and frequency dependency of damping resistance[7,8]

The reaction of viscous dampers is mainly velocity proportional. Slow motion of the piston, for example from a heat expansion in the supported system, leads to nearly no resistance, but in the case of a short pulse or random excitation with a high velocity, the damper will react with a high resistance. Thus, the helical spring-viscous damper isolation systems are capable of providing an effective isolation for both seismic and mechanical vibrations.

EFFECTIVENESS FOR A VIBRATION ISOLATION

The effectiveness of a coil spring-viscous damper system for a vibration isolation of an EDG was demonstrated through a measurement of its vibration during an operation. The vibration measurement for an identical EDG set with different base systems - one with an anchor bolt system and the other with a coil spring-viscous damper system - was conducted. The engine unit of an EDG set to be measured is a model 16PC2-5V 400 (7,650 kW at 514 rpm) manufactured by HANJUNG-SEMT Pielstick. The EDG set is installed on a concrete foundation with anchor bolts (anchor bolt system) at Yonggwang Nuclear Unit 5, while mounted on 20 coil spring units and 6 viscous dampers (spring-damper system) at Ulchin Nuclear Unit 3 of Korea.

Spring Damper System for an Emergency Diesel Generator

The EDG set of Ulchin Nuclear Unit 3 is mounted on a spring-damper system in order to prevent a transfer of an operational vibration from the EDG body to the floor of the building. A spring unit consists of 8 coil spring elements, and has a vertical stiffness of 3.56 kN/mm and a horizontal stiffness of 2.49 kN/mm as shown in Figure 2. A spring unit has a

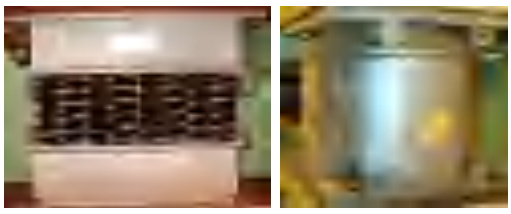

Item		Properties
Load Capacity		178 kN
Height		405 mm
Stiffness	Vertical	3.56 kN/mm
	Horizontal	2.49 kN/mm
Damping Coefficient	Vertical	250 kNs/m
	Horizontal	250 kNs/m

Fig. 2 Spring-damper system for the EDG set

ratio of the horizontal stiffness to the vertical stiffness of 0.7. A viscous damper has a damping coefficient of 2.50 kNs/m in both the vertical and horizontal directions as shown in Figure 2.

Vibration Measurement

As described before, an identical EDG set is installed on a different base system at two different nuclear power plants: one is on the anchor bolt system and the other is on the spring-damper system. The vibration was measured by using 8 PCB Piezotronics model 393B12 accelerometers, whose locations are shown in Figures 3 and 4, during both a non-operation condition and a normal operation condition of the engine for a comparison. For the anchor bolt system, 6 accelerometers (P1-P6) were installed on the surface of the EDG concrete foundation separated from the floor slab, one (P7) was installed on the engine, and one (P8) was installed on the concrete floor slab as shown in Figure 3. For the anchor bolt system, 6 accelerometers (P1-P6) were installed on the steel frame which supports the EDG, one (P7) was installed on the engine, and one (P8) was installed on the concrete floor slab.

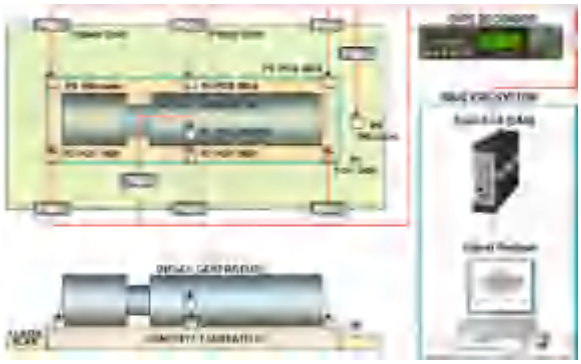

Fig. 3 Vibration measurement system for the anchor bolt system

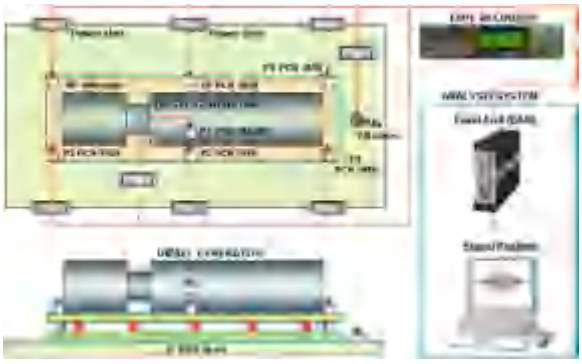

Fig. 4 Vibration measurement system for the spring-damper system

Acceleration Responses

The accelerations measured from the EDG with the anchor bolt system and the spring-damper system during both a non-operation condition and a normal operation condition of the engine are shown in Tables 1 and 2. For the EDG with the anchor bolt system, the average accelerations measured on the concrete foundation (P1-P6) are 0.005 m/s^2 or 53.0 dB under a non-operation condition and 0.166 m/s^2 or 84.0 dB under a normal operation condition. Accelerations on the engine unit (P7) were recorded as 0.183 m/s^2 or 85.2 dB under a non-operation condition and as 1.056 m/s^2 or 100.5 dB under a normal operation condition, and the accelerations on the floor slab (P8) were recorded as 0.003 m/s^2 or 48.0 dB under a non-operation condition and as 0.071 m/s^2 or 77.1 dB under a normal operation condition. A larger acceleration was measured on the engine unit than on the concrete foundation and floor slab. Under a normal operation condition, about 84 and 77 percent of the acceleration on the engine unit was measured on the concrete foundation and floor slab, respectively. There was an 18 percent increase of the acceleration on the engine unit under the normal operation condition, while there was a 60 percent increase of the acceleration on the concrete foundation and floor slab under the normal operation condition. This means that much of the vibration of the engine unit is transmitted to the concrete foundation and floor slab. Considering the accelerations under the non-operation condition, the increase of the acceleration on the floor slab reaches 190 percent.

For the EDG with the spring-damper system, the average accelerations measured on the steel frame (P1-P6) are 0.024 m/s^2 or 67.5 dB under a non-operation condition and 4.262 m/s^2 or 112.2 dB under a normal operation condition. This significant increase on the steel frame is due to the spring-damper system which supports the EDG set and the steel frame. Accelerations on the engine unit (P7) were recorded as 0.036 m/s^2 or 71.1 dB under a non-operation condition and 1.997 m/s^2 or 106.0 dB under a normal operation condition, and the accelerations on the floor slab (P8) were recorded as 0.008 m/s^2 or 58.2 dB under a non-operation condition and 0.048 m/s^2 or 73.7 dB under a normal operation condition. The increase of the accelerations on the engine unit and the floor slab is not significant when compared to the increase for the anchor bolt system. Under a normal operation condition, about 106 and 70 percent of the acceleration on the engine unit were measured on the steel frame and floor slab, respectively. There was a 49 percent increase of the acceleration on the engine unit under the normal operation condition, while there were 66 and 27 percent increases of the acceleration on the steel frame and floor slab under the normal operation condition, respectively. This means that when the engine is in the normal operation, the vibration of the steel frame will be increased by the base isolation system, while the vibration transmitted to the floor slab will be reduced significantly. Considering the accelerations under the non-operation condition, the decrease of the acceleration on the floor slab reaches 44 percent. After all, the reduction of the transmitted acceleration to the floor slab from the engine unit reaches about 80 percent for the spring-damper system when considering the increase on the floor slab for the anchor bolt system.

Figure 5 shows the vibration records measured on the EDG engine unit (P7), the EDG foundation (P1), and the floor slab (P8) for the anchor bolt system during a normal operation condition of the engine. It is found that the vibration amplitude on the EDG foundation is smaller than that on the EDG engine, and the vibration amplitude on the floor slab is smaller than that on the foundation because a direct transmission of a vibration is prevented by the gap between the concrete foundation of the EDG set and the floor slab of the building. The vibration of the EDG foundation may be transmitted to the floor slab through the subsoil and the building foundation. Thus, the gap between the foundation of the EDG set and the floor slab of the building more or less has an isolation effect on the EDG set. Figure 6 shows the vibration records measured on the EDG engine unit (P7), the steel frame (P1), and the floor slab (P8) for the spring-damper system during a normal operation condition of the engine. It is found that the vibration amplitude on the steel frame is significant but the vibration amplitude on the floor slab is negligible because much of the vibration on the steel frame is thoroughly isolated by the spring-damper system. This figure demonstrates the effectiveness of the spring-damper system in isolating a mechanical vibration of rotating machines.

Table 1. Vibration measurement for the anchor bolt system

Measuring Location	Non-Operation				Normal Operation			
	Time Domain		Frequency Domain		Time Domain		Frequency Domain	
	Peak (m/s^2)	Peak* (dB)	OA (m/s^2)	OA* (dB)	Peak (m/s^2)	Peak* (dB)	OA (m/s^2)	OA* (dB)
P1	0.004	52.5	0.0009	39.3	0.187	85.4	0.0672	76.6
P2	0.004	51.3	0.0007	37.4	0.140	82.9	0.0543	74.7
P3	0.006	55.1	0.0011	41.4	0.117	81.4	0.0421	72.5
P4	0.006	56.0	0.0013	42.6	0.269	88.6	0.0880	78.9
P5	0.003	50.0	0.0005	35.1	0.147	83.4	0.0506	74.1
P6	0.005	54.0	0.0009	39.5	0.133	82.5	0.0467	73.4
P7	0.183	85.2	0.0403	72.1	1.056	100.5	0.3619	91.2
P8	0.003	48.0	0.0005	34.8	0.071	77.1	0.0214	66.6

*Reference amplitude = 1×10^{-5}

Table 2. Vibration measurement for the spring-damper system

Measuring Location	Non-Operation				Normal Operation			
	Time Domain		Frequency Domain		Time Domain		Frequency Domain	
	Peak (m/s^2)	Peak* (dB)	OA (m/s^2)	OA* (dB)	Peak (m/s^2)	Peak* (dB)	OA (m/s^2)	OA* (dB)
P1	0.023	67.3	0.0051	54.2	3.202	110.1	1.3599	102.7
P2	0.024	67.7	0.0042	52.6	2.879	109.2	1.3480	102.6
P3	0.031	69.7	0.0075	57.6	6.242	115.9	3.0339	109.6
P4	0.023	67.2	0.0057	55.2	4.807	113.6	2.0520	106.2
P5	0.017	64.6	0.0050	54.1	3.072	109.7	1.3192	102.4
P6	0.027	68.7	0.0055	54.9	5.367	114.6	2.0278	106.1
P7	0.036	71.1	0.0033	50.4	1.997	106.0	0.9339	99.4
P8	0.008	58.2	0.0033	50.5	0.048	73.7	0.0218	66.8

*Reference amplitude = 1×10^{-5}

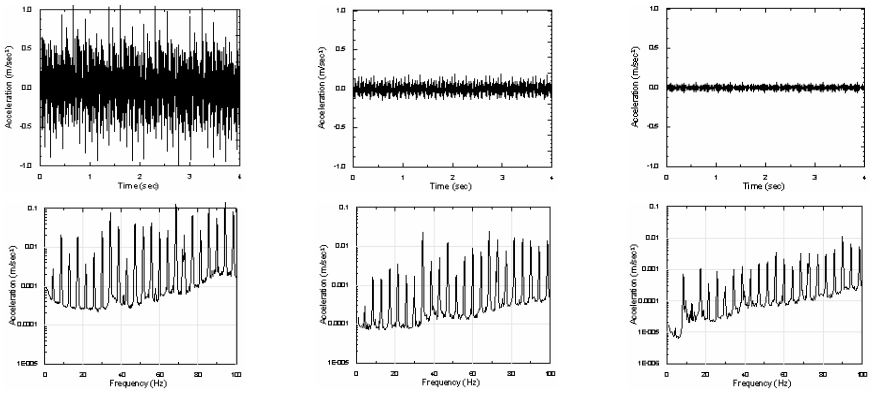

(a) Engine unit (P7) (b) Foundation (P1) (c) Floor slab (P8)

Fig. 5 Vibration records for the anchor bolt system

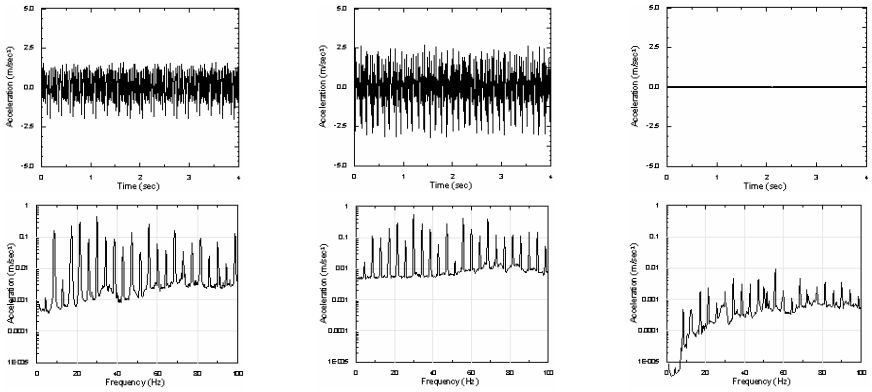

(a) Engine unit (P7) (b) Steel frame (P1) (c) Floor slab (P8)

Fig. 6 Vibration records for the spring-damper system

EFFECTIVENESS FOR A SEISMIC ISOLATION

The seismic effectiveness of a coil spring-viscous damper system was demonstrated by seismic tests of the scaled model of a base-isolated EDG on a shaking table. As a prototype, an EDG set with a HANJUNG-SEMT Pielstick Engine 16PC2-5V 400 was chosen, which is identical to the EDG installed at Yonggwang Nuclear Unit 5 and Ulchin Nuclear Unit 3 of Korea, and the scaled model was designed to represent the seismic behavior of a prototype of the EDG set. Concrete and steel blocks were used to build an EDG model, and a coil spring-viscous damper system was used as a base isolation system. The dynamic characteristics of the coil spring-viscous damper system were obtained by cyclic tests and the seismic responses of the base-isolated EDG model were obtained by shaking table tests.

Test Model

The prototype of the EDG set consists of an engine unit, a generator unit, and a concrete mass. Net weights of the engine unit, the generator unit, and the concrete mass are 912 kN, 392 kN, and 2,474 kN, respectively, and the total weight is 3,779 kN. A 6-DOF seismic simulator with a table dimension of 2.5 m × 2.5 m was used for the model test. Test model was designed by considering the size of the shaking table of the simulator as shown in Figure 7, which consists of a concrete block of 2,300 mm × 800 mm × 450 mm, four steel blocks of 600 mm × 600 mm × 140 mm, and two steel plates of 1,500 mm × 300 mm × 30 mm. Total weight of the test model is 39 kN and the steel blocks were placed to have an equivalent mass center of the prototype.

Spring Damper System for Test Model

For the seismic isolation of the EDG test model, a spring-damper unit that consists of a combination of 2 coil springs and one viscous damper was adapted as shown in Figure 8. The stiffnesses and the damping coefficients of the spring-damper unit for the vertical and horizontal directions were determined by the seismic responses of the EDG test model for the input motion. The test model was supported by 4 spring-damper units as shown in Figure 7.

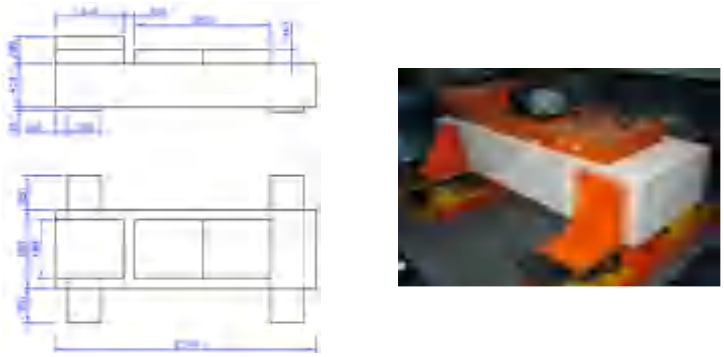

Fig. 7 EDG test model for table tests

Item		Properties
Load Capacity		15 kN
Height		410 mm
Stiffness	Vertical	0.144 kN/mm
	Horizontal	0.04 kN/mm
Damping Coefficient	Vertical	3.5 kNs/m
	Horizontal	4.0 kNs/m

Fig. 8 Spring-damper unit for the EDG test model

Shaking Table Test

Seismic tests were carried out for one and three directional excitations with three peak acceleration levels of 0.1g, 0.2g, and 0.3g. An artificial time-history corresponding to the scenario earthquake for a Korean nuclear site was used as a table input motion. Identical input motions and peak acceleration levels were used in the horizontal and vertical directions. Figure 9 shows the artificial time history and response spectrum of the input motion. The acceleration and displacement responses were measured by using two accelerometers (A1 & A2) and eight LVDTs (D1-D8) as shown in Figure 10.

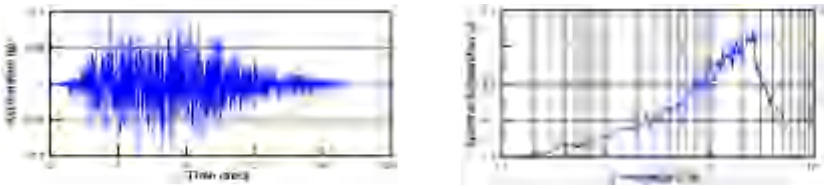

(a) Artificial time-history (b) Response spectrum

Fig. 9 Input motion for the shaking table tests

(a) EDG test model (b) Accelerometers and LVDTs

Fig. 10 Test model and measurement systems for the shaking table test

Seismic Responses

Figures 11 and 12 show the acceleration responses obtained from accelerometer A1 for the peak acceleration levels of 0.1g, 0.2g, and 0.3g during the one and three directional excitations and the spectral accelerations for the peak acceleration level of 0.2g, respectively. Figure 11 shows that the acceleration responses on the EDG model are reduced significantly by the spring-damper system. There is little difference between the acceleration responses in the one horizontal excitation and those in the three directional excitations. Figure 12 shows that identical spectral accelerations are obtained from accelerometers A1 and A2 in both the one horizontal excitation and the three directional excitations, and the predominant frequency shift to 1.3Hz from 23.5Hz. Thus, the spectral accelerations decrease significantly. The differences between the acceleration responses in the one horizontal excitation and the three directional excitations are very small.

The seismic effectiveness of the coil spring-viscous damper system was evaluated by the ratio of the maximum acceleration response for the model to the table acceleration as arranged in Table 3. The average response ratios for the one horizontal excitation, the horizontal and vertical directions for three excitations are 0.283, 0.305, and 0.558, respectively. This indicates that the spring-damper system reduces the seismic force transmitted to the EDG model from the table by

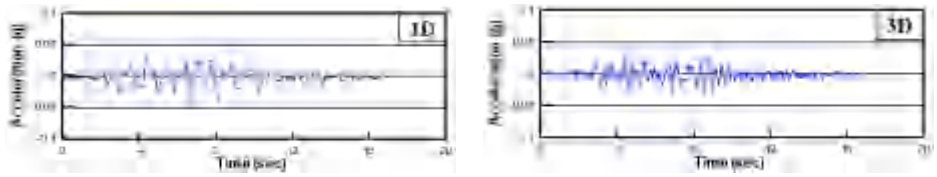

(a) Peak acceleration of 0.1g

(b) Peak acceleration of 0.2g

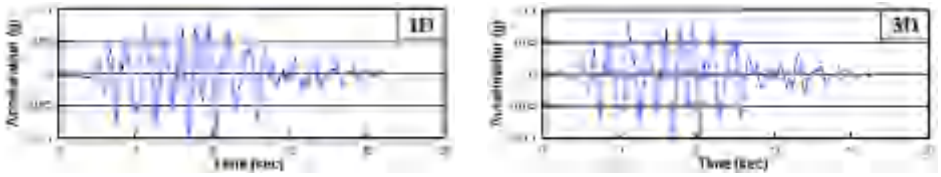

(c) Peak acceleration of 0.3g

Fig. 11 Acceleration responses for different peak accelerations at accelerometer A1

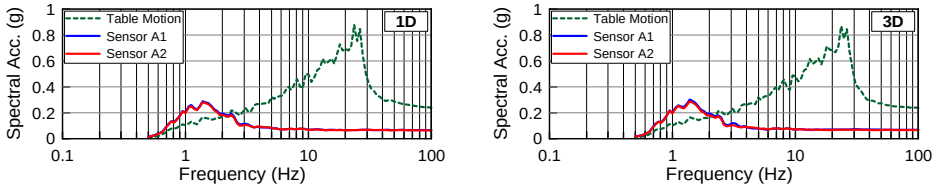

(a) One horizontal excitation (b) Three directional excitations

Fig. 12 Spectral accelerations for peak acceleration of 0.2g

Table 3. Acceleration response ratios for the isolated EDG test model

Target PGA (g)	1D-Horizontal			3D-Horizontal			3D-Vertical		
	Table (g)	Model (g)	Ratio	Table (g)	Model (g)	Ratio	Table (g)	Model (g)	Ratio
0.1	0.118	0.035	0.297	0.110	0.037	0.336	0.062	0.034	0.548
0.2	0.242	0.066	0.273	0.238	0.070	0.294	0.127	0.072	0.567
0.3	0.353	0.098	0.278	0.354	0.101	0.285	0.181	0.101	0.558

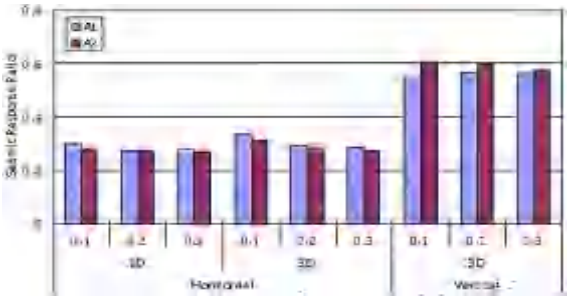

Fig. 13 Comparisons of acceleration response ratios for the isolated EDG test model

up to around 70 percent in the horizontal direction and 45 percent in the vertical direction, respectively. These acceleration response ratios for different acceleration levels are also shown in Figure 13. It is easily seen that the spring-damper system is an effective isolation device for the EDG.

CONCLUSION

The effectiveness of a coil spring-viscous damper system as a vibration and seismic isolation system for an EDG was evaluated in this study. The effectiveness of a coil spring-viscous damper system for a vibration isolation of the EDG was evaluated through a measurement of its vibration during an operation. The vibration measurement for an identical EDG set with different base systems - one with an anchor bolt system and the other with a coil spring-viscous damper system - was conducted. The acceleration responses for the anchor bolt system and the spring-damper system during a non-operation condition and a normal operation condition of the EDG engine showed that the spring-damper system reduces the acceleration amplitude transmitted to the building floor slab from the EDG engine unit by more than 80 percent.

The seismic effectiveness of a coil spring-viscous damper system was evaluated by seismic tests with a scaled model of a base-isolated EDG on a shaking table. The scaled model was designed to represent the seismic behavior of a prototype of the EDG set. The seismic responses of the base-isolated EDG model obtained by the shaking table showed that the spring-viscous damper system could reduce the seismic force transmitted to the EDG by up to 70 percent.

It was demonstrated that a spring-viscous damper is an effective vibration and seismic isolation system for an EDG in nuclear power plants through an evaluation of its vibration and seismic isolation effectiveness. A coil spring-viscous damper system is suitable for vibrating machines to reduce both the transmission of their mechanical vibrations to a floor during an operation and the transmission of a seismic force to them during an earthquake.

ACKNOWLEDGEMENT

This study was supported by the Mid- and Long-Term Nuclear Research and Development Program of the Ministry of Science & Technology, Korea.

REFERENCES

1. Tajirian, F.F., “Base Isolation Design for Civil Components and Civil Structures,” Proceedings of the Structural Engineers World Congress, San Francisco, California, July 18-23, 1998.
2. Malushte, S.R. and Whittaker, A.S., “Survey of Past Base Isolation Applications in Nuclear Power Plants and Challenges to Industry/Regulatory Acceptance,” Transactions of the 18th International Conference on Structural Mechanics in Reactor Technology, paper K10/7, Beijing, China, August 7-12, 2005.
3. Choun, Y.S. and Choi, I.K., “Effect of Seismic Isolation of Nuclear Plant Equipment on Core Damage Frequency,” Transactions of the Korean Nuclear Society Autumn Meeting, Yongpyoung, Korea, October 24-25, 2002.
4. Choun, Y.S., Kim, M.K. and Ohtori, Y., “The Use of a Base Isolation System for an Emergency Diesel Generator to Reduce the Core Damage Frequency Caused by a Seismic Event,” Transactions of the 19th International Conference on Structural Mechanics in Reactor Technology, Toronto, Canada, August 12-17, 2007.
5. Evans, J.B., “Vibration Control for a 25 MW Steam-Turbine Generator Installation near Academic Teaching and Research Laboratories,” Proceedings of the 12th International Congress on Sound and Vibration, Lisbon, Portugal, July 11-14, 2005.
6. Kostarev, V.V., Petrenko, A.V. and Vasilyev, P.S., “An Advanced Seismic Analysis of NPP Powerful Turbogenerator on Isolation Pedestal,” Transactions of the 18th International Conference on Structural Mechanics in Reactor Technology, paper A01/5, Beijing, China, August 7-12, 2005.
7. GERB Schwingungsisolierungen GmbH & Co. KG, Vibration Isolation Systems, 10th Edition, Berlin, Germany, 2000.
8. Huffmann, G.K., “Full Base Isolation for Earthquake Protection by Helical Springs and Viscodampers,” Nuclear Engineering and Design, Vol. 84, 1985, pp. 331-338.

Hybrid Seismic Response Control System for Nuclear Power Station

Satsuya Soda: Professor, School of Science & Engineering, Waseda University
Yoshiaki Komatsu: Manager, Nuclear Facilities Division, Obayashi Corporation

ABSTRACT

Nuclear Power Stations (NPS) should be so designed as the structural and non-structural members not to be subject to slightest damage even if the seismic ground motion is extremely strong. There are two alternative ways to achieve this design purpose. One is to place the station on very hard rock where very small amplification of ground motion is expected. The other is to use a base isolation system to minimize the transfer of the seismic force from the ground to the upper building. In the case of constructing a next generation reactor building on seismically active site, the latter is regarded inevitable. The problem *is* what sort of base-isolation system to apply.

There are already many sorts of base-isolation systems. Though they have been confirmed to be quite effective to let the buildings survive even very strong earthquake ground motions, the number of the base-isolated building has not increased very much, especially the house. One of the reasons can be attributed to that those conventional industrial isolators are a bit too expensive, especially for houses. Therefore, we proposed[1] the use of a less expensive handmade sliding base system for houses. The system consists of, from the bottom to the top, a concrete mat foundation, a polyvinyl chloride sheet and an upper structure with solid base. General view of the lower part of the test structure is shown in a figure at the bottom. We experimentally confirmed that the system yields quite stable load-deflection relation with the friction coefficient of around 0.2. Since the upper structure is actually not ideally rigid, acceleration on the top will be higher than that on the sliding base. So, such high-damping devices as oil dampers or friction dampers are supposed to be used together. We confirmed analytically that, by installing some oil dampers into the upper building, the maximum acceleration of the top of a two or three story house would be no greater than 400 cm/s^2.

We propose here to apply this hybrid seismic response control system with a sliding base and additional damping devices to seismic design of a next generation reactor building. The target maximum acceleration is no greater than 500 cm/s^2. There are lots of things that are quite different from the case of the house. For example, the NPS is so heavy that we use tougher polyethylene terephthalate or ultra high molecular weight polyethylene. In order to let the sliding behavior quite stable, concrete surface is subject to finishing. There might be some rotational vibration around the vertical axis caused by such non-uniform distribution of the friction and the mass. In relation to this, it was confirmed in the previous study that excessive rotation could be avoided by installing some mechanical links between the foundation and the base of the upper building as shown in the figure below. In the new system, mechanical link is replaced by hydraulic links, which are expected to be used as oil jacks to remove the residual displacement after very strong ground motion.

This study aims at showing the prospect of making use of the proposed sliding base-isolation system in the seismic design of NPS. The study consists of three parts as follows.

1) Feasibility study on availability of a proposed hybrid seismic response control system.
2) Experimental study on the mechanical properties of the sliding base made up of grinded concrete surface and high polymer sheet.
3) Analytical study on the seismic behavior of a structural model of NPS with base-isolation system consisting of sliding base and extra oil and friction dampers in the upper building.

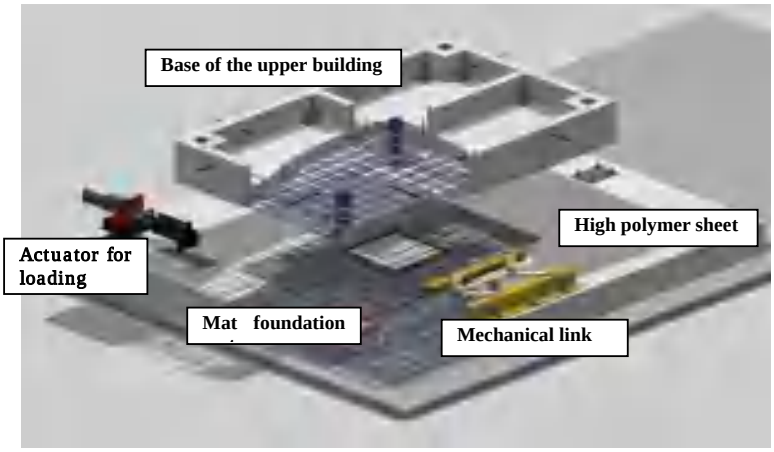

General view of the test structure of the sliding base for houses[1)]

INTRODUCTION

In Japan, a demonstration plant and a commercial plant of an FBR are planed to be in operation in 2025 and in 2050 respectively. In order that those plants be free from any slightest damages even when subject to intense seismic ground motion, use of a base-isolation system is taken for granted. Since we have had some strong ground motions recently, Japanese regulatory guide for seismic design of NPS is now extensively reviewed and the intensity of seismic design ground motion is very likely to become much higher than that prescribed in the current guide. Therefore, most structural engineers understand that for economy's sake the whole NPS has to be base-isolated in the horizontal direction. They think that the primary heavy component can be vertically base-isolated by means of specially installed devices or systems.

The first part of the study consists of two preliminary analyses. The analysis using a single degree of freedom (SDOF) rigid body model with a rigido-plastic element to represent the sliding base indicates that the sliding base really works to isolate the upper building structure from the ground motion. Important thing to note is that the system may accompany quite a lot of shifted and hence the residual displacement during a strong ground motion. It also includes the analysis by multi-degrees of freedom (MDOF) model to investigate the effect of acceleration amplification from the base to the top of the structure. Based on these analytical results, proper value for the friction coefficient for the sliding base is identified to be among 0.1 to 0.2. It is also suggested that some additional damping devices have to be installed if we want the maximum acceleration at the top of the structure be less than 500 cm/s^2. The second part deals with the experimental study to find out the combination of materials to yield the identified proper friction coefficient. We noticed that good quality concrete could easily be grinded as smooth as the polished marble stone and we found out that the sliding between the grinded concrete surface and such high polymer materials as polyethylene terephthalate or ultra high molecular weight polyethylene (UHMWPE) yield friction coefficient that we wanted. The last part describes another analytical study to show that the proposed hybrid structural system is useful to reduce maximum acceleration at the top without excessive displacement at the bottom.

FEASIBILITY ANALYSIS OF THE PROPOSED STRUCTURAL SYSTEM

Seismic Response of a SDOF Model

A simple SDOF model shown in Fig. 1 is used in the analysis to show how the sliding base works. Load-deflection relation of the sliding base is assumed to be an ideal rigid-plastic one as shown in Fig. 2. Sliding force changes depending on the friction coefficient μ of the sliding base. Original ground motion record of the NS component of 1995 Hyogo-ken Nanbu Earthquake (Kobe_NS) is used in the analysis. Four different values of friction coefficient are tested, ranging from 0.1 to 0.4. Displacement time histories in Fig.3a show that they accompany unstable drift and corresponding residual displacement. The maximum displacement seems not so sensitive to the friction coefficient and is as great as nearly 30 cm, as is usually expected in the normal base-isolated building with rubber bearings and dampers. Although the displacement seems quite unstable, maximum acceleration is almost precisely in proportion to the friction coefficient as seen in Fig. 3b. This result suggests that the sliding base is useful to cut off the transmission of seismic force from the base to the upper buildings. However, some proper measure has to be taken into consideration to deal with the possible residual displacement after intense ground motion.

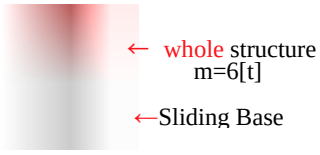

Fig. 1 Parameters for Model

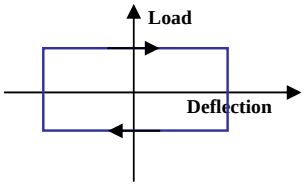

Fig. 2 Load-deflection relation of sliding base

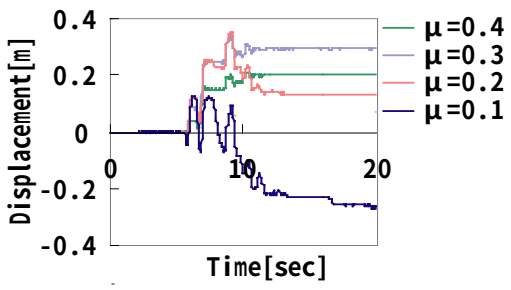

a. displacement

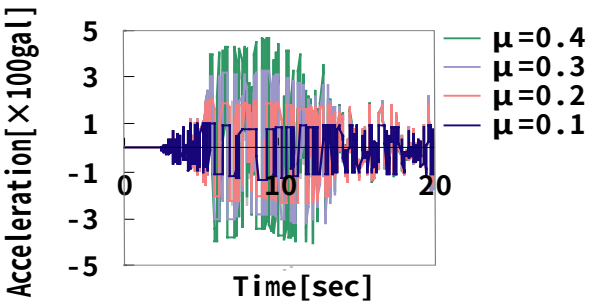

b. acceleration

Fig. 3 Displacement and acceleration time histories

Seismic Response of a MDOF Model

In this section, three and four degrees of freedom models are used. The former is to represent normal structural system fixed to the ground and the latter, the one rested on a sliding base. The four degrees of freedom model consists of one mass for sliding base and the three masses for the upper building to take into consideration the acceleration amplification from the bottom to the top. Yield strength of the sliding base is the friction coefficient times the total weight of the model including sliding base. The mass are listed in Table. 1. The load-deflection relations of the upper structure stories are assumed to be bi-linear ones as listed in Table 2. Natural period and mode vectors are shown in Fig. 5. Inherent damping property of the upper structure is assumed to be 2% for the first mode when the super structure alone is subject to vibration. In this analysis, four different structural systems are compared. First one corresponds to the normal one that has neither sliding base nor any extra damping devices. Next one has no sliding base either but additional viscous dampers are installed. The third one has a sliding base without damping devices. The last one corresponds to a proposed hybrid seismic response control system with a sliding base and damping devices in the upper building. Amount of the extra viscous dampers is changed according to the damping factor from 0.1 to 0.3 for the first natural mode. Fig. 6a compares the maximum story deflection when subject to the original Kobe_NS ground motion. Fig. 6b compares the maximum acceleration. Broken lines correspond to the case of no extra viscous damping devices and the solid lines the case with the dampers. We can see that by placing the upper building on a sliding base, both the maximum deflection and the maximum acceleration can be significantly reduced. But, in order to let the maximum response be no greater than 400-500 cm/s^2, we install some extra damping devices into the upper structure.

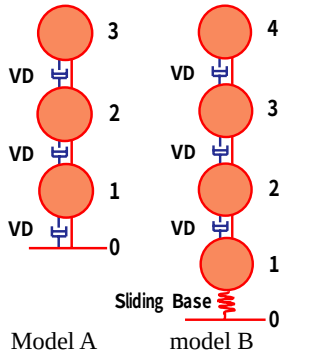

Model A model B

Fig. 4 Normal structural system model A (left) and proposed hybrid system model B (right)

Table 1 Mass data

	m1 Sliding Base	m2 2nd Floor	m3 3rd Floor	m4 Top Floor
mass[t]	0.05816	0.01432	0.01432	0.01068

Table 2 Mechanical properties of model A

story	1st Stiffness [kN/m]	2nd Stiffness [kN/m]	Yield Point [kN]
3	86.75	0.694	0.39
2	88.34	0.70672	0.39
1	92.31	0.73848	0.39

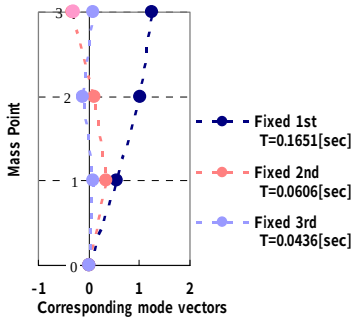

Fig. 5 Natural period and corresponding mode vectors of model A

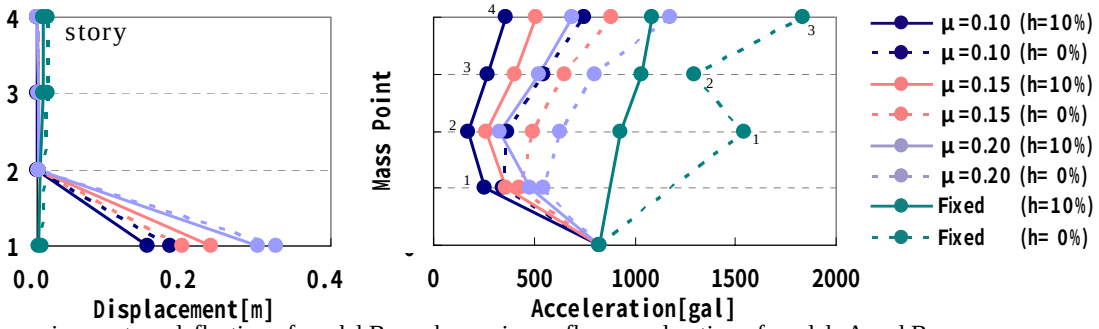

a. maximum story deflection of model B b. maximum floor acceleration of models A and B

Fig. 6 Comparison of maximum response

Fig. 7 is prepared to see how the coefficient of friction of the sliding base and the damping property of the upper structure work together to decrease the maximum acceleration of the top of the building. As is mentioned in the introduction, our primary concern is to let the maximum acceleration in the upper building be no greater than 400-500 cm/s^2. So, it is concluded that the proposed hybrid seismic response control structural system could be realized by the use of both the sliding base with the friction coefficient of 0.1–0.2 and the extra damping devices corresponding to the equivalent first mode damping factor of 20-30%.

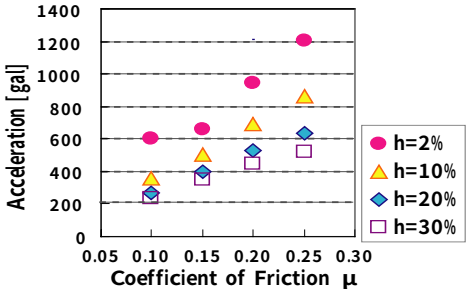

Fig. 7 Max acceleration of the top floor

EXPERIMENTAL STUDY TO IDENTIFY IDEAL SLIDING SYTEM

Outline of Experiment

This section describes the experimental study to find out proper sliding system with the friction coefficient ranging from 0.1 to 0.2. One important thing we want to achieve is to get far less expensive sliding system than those conventional industrial sliding isolators. Our preliminary test showed that good quality concrete could easily be finished very smooth. So, finely grinded concrete is chosen as one side of the friction surface. As the other side of the friction surface, we use ultra high molecular weight polyethylene (UHMWPE) and barium ferrite coated polyethylene terephthalate (BaFe). Effect of the degrees of roughness of the concrete surface is investigated. Other important parameters considered in the experiment are the loading velocity and the pressure on the sliding surface.

Figure 8 shows the loading system. Concrete plate is fixed to the base beam. Four pieces of UHMWPE block or BaFe sheet are bonded to the steel plate as the slider. Zero to five pieces of 5 kg weights are used to let the friction surface be subject to six different compressive stress. In the case that sliding sheet is spread all over between the mat foundation and the concrete base of a full scale normal NPS, the pressure is supposed to range from 0.2 to 0.4 MPa. In order to investigate the effect of the loading velocity, various combinations of different amplitude and frequency are used in the test as listed in Table 3.

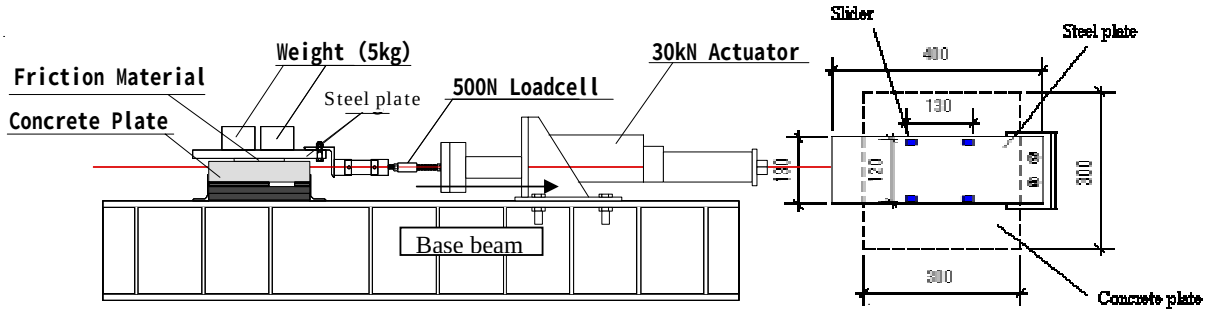

Fig. 8 Loading system (left) and arrangement of piece of sliding sheet or block on the friction surface (unit: mm)

Test Results

Effect of the roughness of concrete surface

Figure 9 shows the effect of the roughness of the concrete surface. In this test, 0.1 Hz sine wave displacement is applied. In the case of using UHMWPE, if there is no grinding, friction is unstable, but some grinding finish seems to make friction property quite stable.

Table 3 Loading parameters

Frequency[Hz]	Amplitude[mm]	Roughness	Surface pressure(kN/m^2)	Weight
0.1	10	not grinded	153.56	none
0.5	20	#24	216.06	1piece
1.0	30	#60	278.56	2pcs.
		#120	341.06	3pcs.
		#240	403.56	4pcs.
		#400	466.06	5pcs.
		#600		

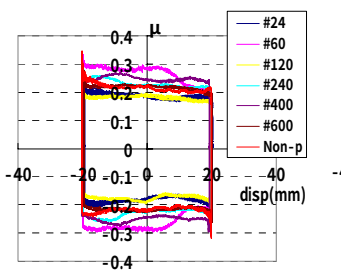

UHMWPE

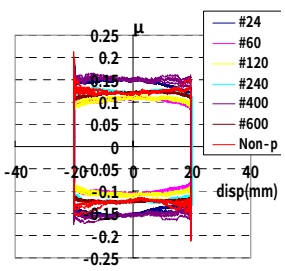

BaFe

Fig. 9 Effect of roughness of concrete surface on coefficient of friction (sine wave 0.1Hz, 0.28MPa)

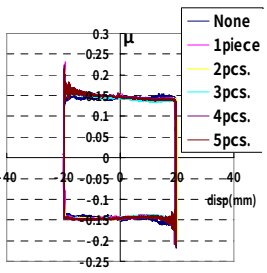

UHMWPE

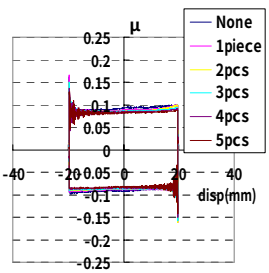

BaFe

Fig. 10 Hysteresis of coefficient of friction (triangular wave, 0.1Hz, #24, 0.28MPa)

Effect of the pressure

Figure 10 compares the effect of compressive stress on the load-deflection relation of the sliding surface. In this test, roughness of the concrete surface corresponds to a #24 grinder. We can see that the all load-deflection relations are quite stable and almost the same regardless of the magnitude of the stress.

Effect of the long term loading

This test is performed to see if the load-deflection relation of the sliding base deteriorates when subject to large amount of cumulative displacement. Analytically expected cumulative displacement for single intense ground

motion is around 10m. Fig. 11 compares the coefficient of friction at the beginning of the loading and at the end of every 10m cumulative displacement. Test results show that we do not have to worry about the deterioration of the sliding surface. Since the existing pressure on the sliding base would be less than 1/100-1/50 of the yielding stress of UHMWPE and BaFe, there would be no need to take creep deflection into consideration.

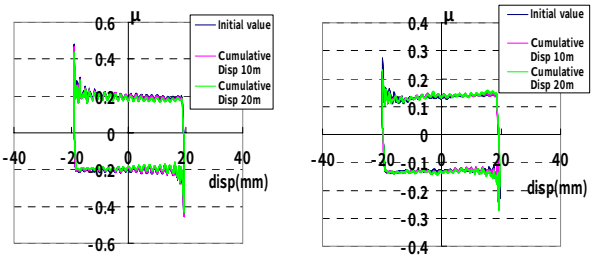

UHMWPE BaFe

Fig. 11 Hysteresis of coefficient of friction (triangular wave, 0.1Hz, 0.28MPa, not grinded)

ANALYTICAL STUDY ON HYBRID SEISMIC RESPONSE CONTROL OF NPS

Structural Model

In this analysis, four and five degrees of freedom shear models are used to represent a sample structural model[2]. The former is used for normal building structure and the latter a hybrid one with sliding base and extra damping devices In Table 4, the node 1 corresponds to the sliding base. Friction coefficient is assumed to be 0.1. Mechanical properties of the analytical model are also listed in Table 4. In the table, the term BL stands for the bilinear element to represent load-deflection relation of the fifth steel frame story. It is also used to represent the frictional property of the sliding base. MTK is the abbreviation for the modified Takeda model to represent reinforced concrete element of the first through the forth story. First and second yield points of the MTK element correspond to concrete cracking strength and yielding of steel reinforcement respectively. Natural damping property of the main structure is assumed to be 2% for the first mode. In the case that the sliding base is applied, viscous and friction damping device is installed in the top steel frame story to get less maximum acceleration. The same original Kobe_NS ground motion as in the previous analyses is used.

Table 4 Mechanical properties of structural model

Floor and Story	Structure	mass [t]	Hysteresis Characteristic	1st Stiffness [kN/m]	2nd Stiffness [kN/m]	3rd Stiffness [kN/m]	1st Yield Point [kN]	2nd Yield Point [kN]	Stiffness Chanfe [%]
5	Steel	5.12E+03	BL	4.52E+06	4.52E+03		9.00E+04		
4	RC	8.48E+03	MTK	4.52E+07	1.13E+07	4.52E+05	6.13E+04	1.84E+05	-20
3		9.98E+03		6.92E+07	1.73E+07	6.92E+05	9.38E+04	2.81E+05	-20
2		9.79E+03		8.91E+07	2.23E+07	8.91E+05	1.21E+05	3.62E+05	-20
1		9.42E+03		1.05E+08	2.63E+07	1.05E+06	1.25E+05	4.28E+05	-20
Isolation		2.34E+04	BL	1.00E+09	1.00E-02		*		

Results and Discussions

Figure 12 shows the displacement time history of the sliding base. Drifted and residual displacement is quite significant. It looks unstable, but the load-deflection relation is quite stable as seen in Fig. 13. Fig. 14 compares the load-deflection relations of the first story of the building model when it is fixed to the ground and when it is placed on the sliding base. Although the strength of the first story is more than half of the total structural weight, the fixed building may be subject to quite amount of structural damage. However, when the building is placed on the sliding base, the first story remains almost elastic. From figures 12-14, it can be said that the upper building is free from damage in compensation for the large displacement of the sliding base including the residual displacement.

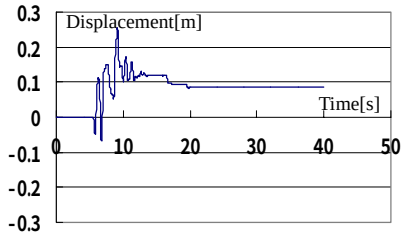

Fig.12 Displacement time history of sliding base

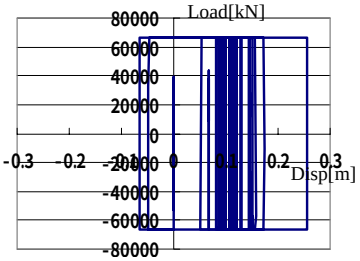

Fig.13 Load-deflection relation of sliding base

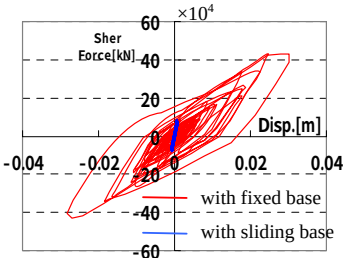

Fig.14 Load-deflection relation of first story

Even when the sliding base is installed, acceleration increases from the sliding base to the top. Broken line in Fig.15 shows that the acceleration of the top floor can not be reduced much if there is sliding base alone and no damper is installed in the top steel frame story. Whereas, when some extra oil dampers are installed in the fifth steel frame story, the acceleration at the top would be no greater than 500 cm/s^2 as shown by solid line. Fig.16 compares acceleration time histories of the top floor of the building with and with out hybrid seismic response control system. Broken line

corresponds to the fixed building structure and solid line the hybrid building structure. It can be concluded that proposed hybrid structural system is quite effective to reduce the maximum acceleration of the upper building.

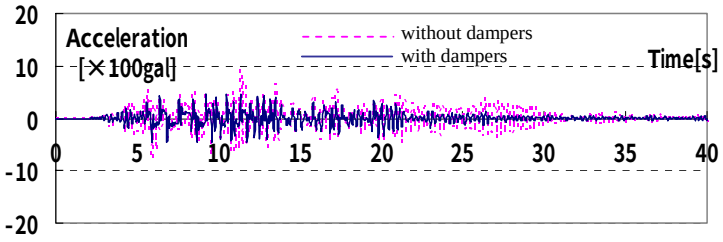

Fig.15 Acceleration time history at the top of hybrid structure with/without oil dampers

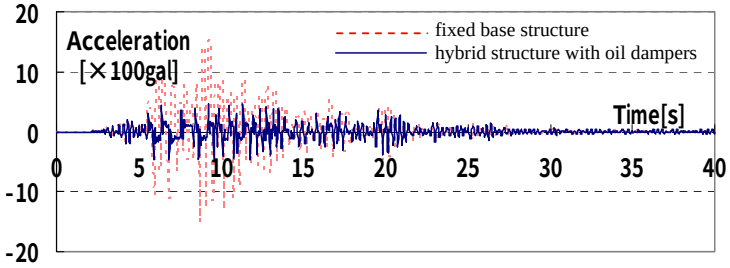

Fig.16 Acceleration time history at the top of fixed base structure and hybrid structure

Fig.17 compares load-deflection relations of the top steel frame of the hybrid structure with and without oil dampers. Fig.18 corresponds to the case that friction dampers[3] are used instead of oil dampers. In this case, strength of the friction damper is set to 30% of the steel frame's weight. Both dampers seem to work almost the same. Fig. 19 compares the acceleration when oil dampers are used with when friction dampers are used instead. Time histories do show some difference, but the maximum accelerations are almost the same.

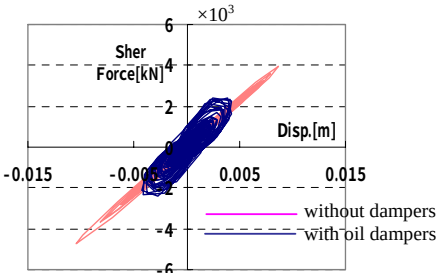

Fig.17 Load-deflection relation of top story with and without oil dampers

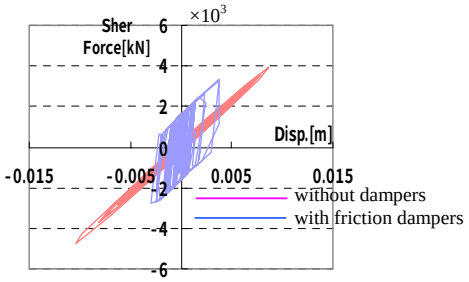

Fig.18 Load-deflection relation of top story with and without friction dampers

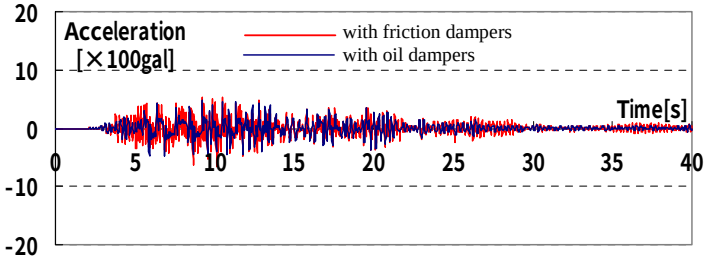

Fig.19 Acceleration time history of the top of the hybrid structure with oil dampers and friction dampers

Hydraulic Link[4]

Since the mechanical properties of the building including the sliding base is not always uniform, there would be some rotation about the vertical axis and even some residual displacement after strong ground motion. We do not think that rotation or residual displacement cause undesirable seismic effects on the building. But they should be removed

before the next strong ground motion. We are thinking of installing hydraulic link systems[4] between the foundation and the base of the upper building instead of the mechanical link shown in the figure on the first page. The links not only work to prevent the rotation of the sliding base but also be used as the jacks to remove the residual displacement.

CONCLUSIONS

Important findings in the study are as follows:
1) Sliding base works to cut off the transmission of seismic force from the mat foundation to the base of the upper building. It often accompanies residual displacement which should be removed after intense ground motion.
2) Sliding base alone does not work to let the maximum acceleration in the upper building be no greater than 400-500 cm/s^2. Proposed hybrid seismic response control structural system could be realized by the use of both the sliding base with the friction coefficient of 0.1–0.2 and the extra damping devices corresponding to the equivalent first mode damping factor of 20-30%.
3) Grinded surface of good quality mat concrete could be used as one side of the friction surface. Such high polymers as ultra high molecular weight polyethylene and barium ferrite coated polyethylene terephthalate are identified to be the other side of the friction surface, exhibiting coefficient of friction around 0.1-0.2. There is no need to worry about the deterioration of the sliding surface and the creep deflection of the polymers.
4) Even when the sliding base is installed, acceleration increases from the base to the top of the building. But, the top acceleration would be no greater than 500 cm/s^2 when some extra oil dampers or friction dampers are installed in the top steel frame of an NPS building.

ACKNOWLEDGMENT

The research was conducted as part of the 2004-2008 Hi-Tech Research Project funded by the Ministry of Education, Culture, Sports, Science and Technology (Title: Structural and performance evaluation technologies to upgrade the earthquake disaster prevention system of the metropolis. Representative: Satsuya Soda). This is also supported by 2005-2007 Grant-in-aid for Scientific Research B (Title: Seismic strengthening design of existing buildings with viscous damping devices. Representative: Satsuya Soda). We would like to express our appreciation to Mr. Jun Sonoda and Miss Emi Miyamoto for preparing the figures and tables in this paper.

REFERENCES

[1]Satsuya Soda et. al., “Development of a wide use base-isolation system for house (Part 1: Outline of a base-isolated platform and analytical study, Part 2: Experimental study on full scale base-isolated platform),” Proceedings of annual conference of AIJ 2005, pp. 789-792
[2]Koshiro En et. al., “A STUDY ON ASEISMIC PERFORMANCE ESTIMATION OF A NUCLEAR FACILITY FROM A VIEW POINT OF STRUCTURAL STABILITY,” J. Struct. Constr. Eng., AIJ, No. 581 pp.23-30, Jul., 2004
[3]Takeshi Sano et. al., “Development of Friction Damper using High Tension Bolts – Experiment on Brake Damper and Application to Building -,” Report of Obayashi Corporation Technical Research Institute, No. 62, 2000, pp. 13-20
[4]Satsuya Soda et. al., “Effectiveness of Linked Oil Dampers in Seismic Response Control,” Proceedings of annual conference of AIJ 2007, in print

Seismic Behaviour Analysis of Dissipation Devices and Assessment of European Shaking Tables and Reaction Walls

Rogerio Bairrao[1)], M.J. Falcao Silva[1)], F. Javier Molina[2)] and Panayotis Carydis[3)]

1) Laboratório Nacional de Engenharia Civil (LNEC), Lisbon, Portugal
2) European Comission, JRC/IPSC/ELSA, Ispra, Italy
3) National Technical University of Athens (NTUA), Athens, Greece

ABSTRACT

The results presented in this paper were achieved within the NEFOREEE research network (New Fields of Research in Earthquake Engineering Experimentation) [1] funded by the European Commission. This network has inherited a big experience from previous consortia of European laboratories working in the field of earthquake and dynamic experimental research and operating paramount European shaking tables and reaction walls.

Benchmark tests were developed on similar specimens at three different facilities (first in Greece, then in Italy and finally in Portugal). A one-degree-of-freedom full-scale steel frame, very easy to put up and to transfer from lab to lab was built. This frame was designed to allow also a relatively smooth assemblage and exchange of two different types of dissipation devices: a shear panel with hysteretic behaviour [2] and a standard industrial shock absorber.

Following a dynamic analysis of the bare frame, a series of tests, for both types of dissipation devices, was performed in each lab. These tests have included an El Centro input, 0.2g peak scaled, sinusoidal excitations for 0.05g and 0.1g, with 80% and 100% of the natural frequency for each specimen configuration and, finally, successive EC8 artificial time histories up to 1g of peak table acceleration.

The last tests concerning this task of the NEFOREEE research network were recently accomplished in Lisbon. So, the main results obtained are included in the present paper thus extending the analysis started in two previous presentations [3,4].

INTRODUCTION

In this experimental program, three of the major European facilities in the earthquake engineering research were involved: JRC (Ispra, Italy), LNEC (Lisbon, Portugal) and NTUA (Athens, Greece).

To perform these benchmarking studies it was necessary to design a single degree of freedom specimen exhibiting a considerable flexibility, to be used in different facilities for a better comparison between shaking table and reaction wall tests. Steel was the main material used to build the model, because it allows a good flexibility and an easy design of the connection details. The specimen had to satisfy some requirements in order to optimise its design and to obtain a better modularity to be used in the different experiments performed in the laboratories that were chosen. The main requirements to be fulfilled were:

1 The dimensions in accordance with the characteristics of the shaking tables and reaction walls to be suitable for both kind of experiments;

2 The total mass not exceeding the maximum capacity of the smallest shaking table involved, in this case 10ton which corresponds to the maximum specimen weight for the NTUA shaking table;

3 The slab, constituted by a metal container filled with concrete and properly connected, designed to achieve the requested mass, not blocking the connections with the frame and allowing future slabs adding to increase the number of the degrees of freedom;

4 The braces with K and X shapes allowing the placement of passive-control devices and a range of natural frequencies convenient for shaking table and pseudo-dynamic tests.

SPECIMEN AND DISSIPATION DEVICES

The main elements of the specimen were designed through an elastic analysis using the finite element program SAP200NL [5] considering two earthquake time history accelerations: one is an earthquake generated to be in accordance with type 1 of the Eurocode 8 [6] and the other is an El Centro earthquake record, both of them with a peak ground acceleration of 0.5g.

According to the design requirements, the frame should present a longitudinal size of 300 cm; a transversal size of 275 cm; a column height of 450 cm; and an inter-storey distance of 300 cm. In what regards the height of the column and the inter-storey distance, the slabs could be spaced with 3m, allowing another steel-concrete composite slab to be added at a height of 6m. Consequently a second degree of freedom can be obtained simply through the use of elements with the same characteristics and details of the basic structure.

A one degree-of-freedom full-scale shear type K-braced steel frame, easily transportable from lab to lab, was conceived [7]. The structure was designed to allow two types of dissipation devices to be inserted: a special shear panel device and a usual industrial device. The model without the energy dissipation devices included presented a very linear behaviour with a very low damping. This should certainly put in evidence the alteration introduced by the testing methods such as control delays in the PsD method or spurious rocking on the shaking table. With non-linear dissipator devices, those deficiencies may be hidden by the large damping developed at the specimen, but an appropriate strain-rate effect compensation technique is necessary within the PsD method. In a similar way, that non linearity may impose limitations as well on the compensation techniques based on linear filtering of the reference signal and traditionally used at the shaking tables [4]. The following figure shows a global view of the specimen just before the experimental program at the LNEC facility:

Fig. 1 – Specimen
on the LNEC 3D shaking table

The structure was equipped with energy dissipation devices in the longitudinal direction. In particular, two dampers have been designed for the purpose. The first one was a steel shear panel [2]; it is inserted into a square steel tube and dissipates energy by means of elastic-plastic shearing. The second type of device tested was a Jarret shock absorber relying on the compression of a viscous-elastic silicone fluid. These devices were applied to the specimen to dissipate a large part of the kinetic energy generated in a seismic event. Both, Dorka and Jarret devices, are shown in Figures 2 and 3.

Fig. 2 - View of the
Dorka shear panel devices

Fig. 3 - View of a
Jarret viscous fluid damper

INSTRUMENTATION

The instrumentation set-up that was used to measure the response of each specimen to earthquake tests on the shaking table is shown in Figures 4 (SPECIMEN I – Bare Frame) and 5 (SPECIMEN II – Frame with Dorka devices and SPECIMEN III – Frame with Jarret devices). In the instrumentation of the specimen were used accelerometers, inductive displacement transducers (LVDTs) and optical displacement transducers (Hamamatsu). The instrumentation used in LNEC was adapted from the instrumentation previously used in JRC and NTUA.

Three accelerometers (A1X, A2X, A3X) were fixed on the top of the specimen in order to measure in and out-of-plane accelerations. Absolute displacements at the top (D3, D4) and at the bottom (D1, D2) level of each specimen were measured with respect to a stiff frame, which was fixed outside the shaking platform. Strain gauges (SG1, SG2) were also used in order to check the strain level at the bottom of steel columns. For the tests performed on SPECIMENS II and III the shear force was measured directly on dissipation devices (LC), while two additional displacement transducers were mounted at the devices as well.

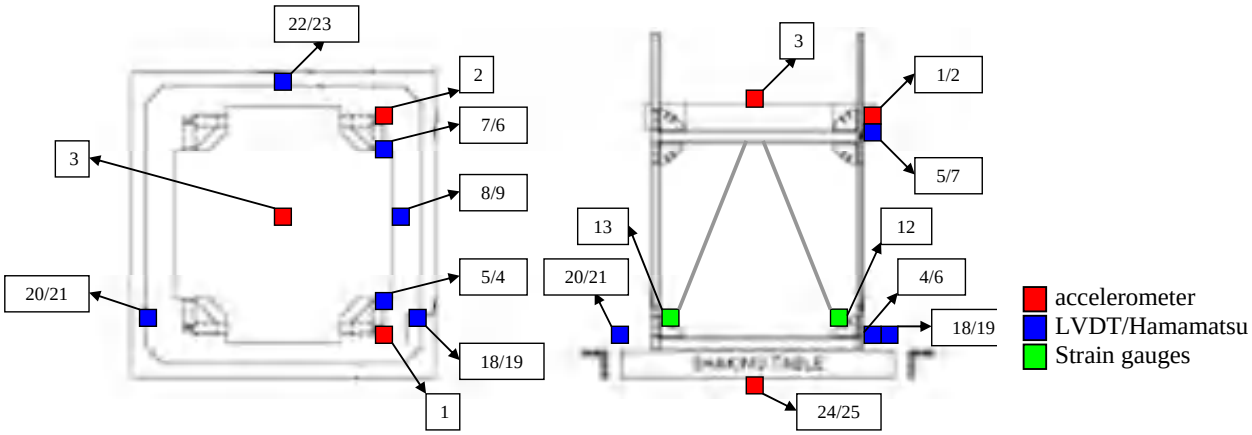

Figure 4 – Instrumentation set-up of SPECIMEN I at LNEC: a) Plan view and b) Elevation.

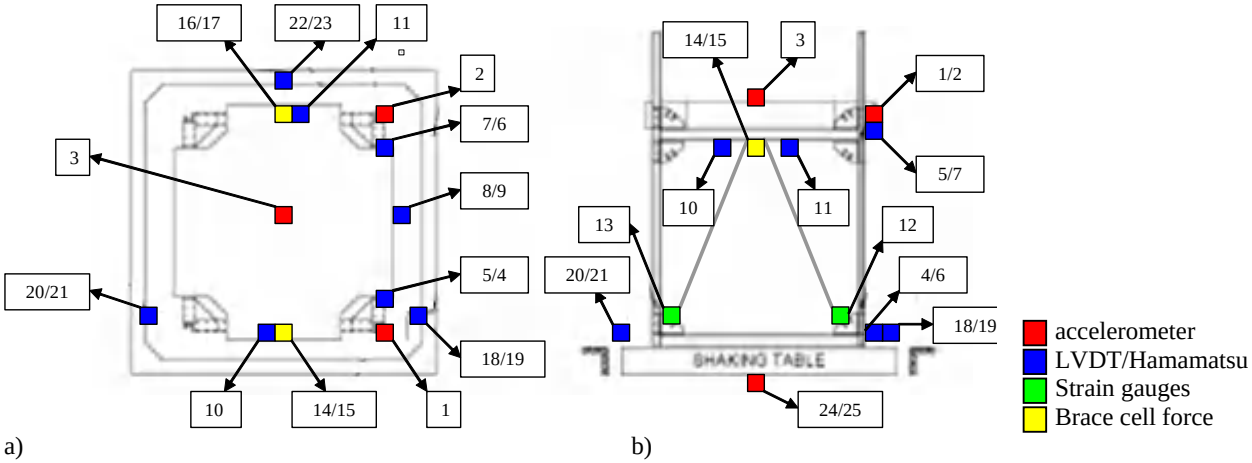

Figure 5 – Instrumentation set-up of SPECIMENS II and III at LNEC: a) Plan view and b) Elevation.

The different sensors were connected to 4 posts corresponding, respectively to: Post 1 – accelerometers, Post 2 – inductive displacement transducers, Post 3 – strain gauges and Post 4 – optical displacement transducers.

EXPERIMENTAL PROGRAM

The loading sequence used in LNEC was very similar to the used in the NTUA tests and was pre-defined for the partners involved in the project. In a similar way to the case of the shaking table tests, the testing campaign at JRC has included some preliminary low-amplitude tests, such as modal tests, by using an instrumented impact hammer, and snap-back tests, at which an initial displacement was introduced after which the structure was left to oscillate freely.

The sequence of tests performed in LNEC tests are presented in the following tables:

Table 1 - **Tests performed on SPECIMEN I (Bare Frame)**

Test	Description
1	Cat00 along EW direction, Table acceleration 0.05g
2	El Centro earthquake along EW direction, Table Acceleration 0.20g
3	Cat01 along EW direction, Table acceleration 0.05g

Table 2 - **Tests performed on SPECIMEN II (Frame with Dorka devices)**

Test	Description
4	Cat02 along EW direction, Table acceleration 0.05g
5	El Centro along EW direction, Table acceleration 0.20g
6	Sinusoidal 10.28 Hz, Table acceleration 0.05g
7	Artificial EC8 time history along EW direction, Table acceleration 0.20g
8	Sinusoidal 8.22 Hz, Table acceleration 0.05g
9	Cat03 along EW direction, Table acceleration 0.05g
10	Artificial EC8 time history along EW direction, Table acceleration 0.60g
11	Cat04 along EW direction, Table acceleration 0.05g
12	Artificial EC8 time history along EW direction, Table acceleration 0.80g
13	Cat05 along EW direction, Table acceleration 0.05g
14	Artificial EC8 time history along EW direction, Table acceleration 1.0g
15	Cat06 along EW direction, Table acceleration 0.05g

Table 3 - **Tests performed on SPECIMEN III (Frame with Jarret devices)**

Test	Description
16	Cat07 along EW direction, Table acceleration 0.05g
17	El Centro along EW direction, Table acceleration 0.20g
18	Sinusoidal 9.48 Hz, Table acceleration 0.05g
19	Artificial EC8 time history along EW direction, Table acceleration 0.20g
20	Sinusoidal 7.58 Hz, Table acceleration 0.05g
21	Cat08 along EW direction, Table acceleration 0.05g
22	Artificial EC8 time history along EW direction, Table acceleration 0.60g
23	Cat09 along EW direction, Table acceleration 0.05g
24	Artificial EC8 time history along EW direction, Table acceleration 0.80g
25	Cat10 along EW direction, Table acceleration 0.05g
26	Artificial EC8 time history along EW direction, Table acceleration 1.0g

The tests performed in LNEC have comprised Stage Tests and Characterisation Tests. The Stage Tests corresponded to main earthquake series with increasing intensities from 0.2 up to 1.0g. These series were uniaxial earthquake records and two different time histories in the main direction (X) were applied. These time histories were, as already referred, a modified component of an El Centro earthquake record and an artificial time history, which was generated to match the elastic response spectrum Type 1 of Eurocode8 [6] with corresponding peak ground acceleration of 0.5g, damping at 5% and a subsoil type A.

The Characterisation Tests have comprised sin-sweeps and “Cat Tests”. The first one corresponded to the performance of a complementary ramp sinusoidal excitation with test frequency 100% and 80% of the natural frequency of the specimen in order to achieve each specimen resonant response. This way just before the earthquake tests the specimen was tested under sine logarithmic sweep excitation along X direction for the determination of its natural frequencies and their damping.

This sine logarithmic sweep signal was in a frequency range of 1 to 35 Hz at a rate of one octave per minute. The tests were executed along global X axis with an amplitude vibration of 0.05g.

There were also performed the "Cat Tests" which preceded every Stage Series and corresponded to low amplitude, broadband base signals with the objective of estimating the specimen's dynamic characteristics and their evolution during the experimental tests. In Figures 6 and 7 are presented the spectra of the time histories used in LNEC.

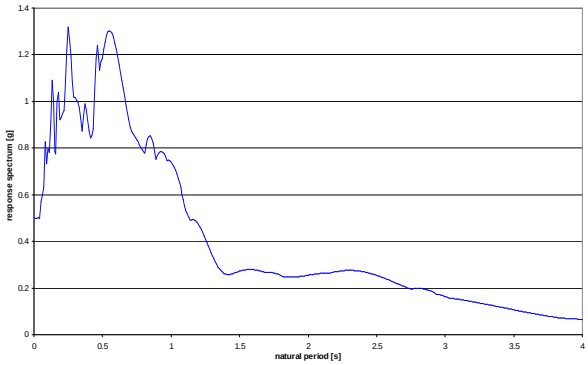

Fig. 6 - Response spectrum for El Centro earthquake (1940) (adapted from [7])

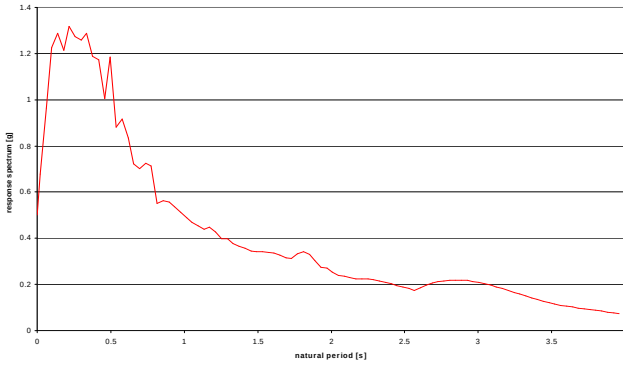

Fig. 7 - Response spectrum for an artificial earthquake according to type 1 of Eurocode 8 (adapted from [7])

TEST RESULTS

The modal frequencies were identified using frequency response functions estimations and the peak picking method. It was identified one translational single mode as a result of the dynamic action imposed for each characterization (cat) series. The evolution of the modal frequencies during the experimental program is presented in Figure 8.

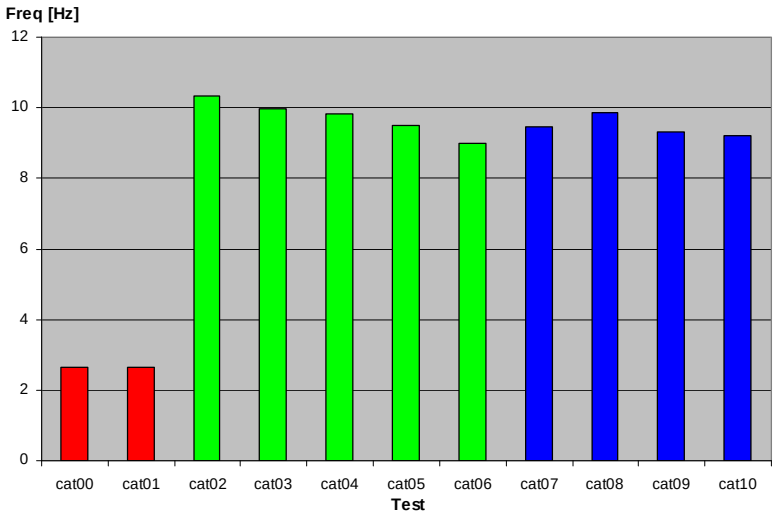

Fig. 8 – Experimental modal frequencies

An example of the identified frequency response functions obtained during the experimental program is presented in Figure 9 for the case of the viscous fluid dampers and after an artificial EC8 input with a shaking table peak acceleration of 0.8g. The damping was estimated for all the specimens, being obtained approximated values of 1.5%, 3% and 7.5% for SPECIMEN I, II and III, respectively.

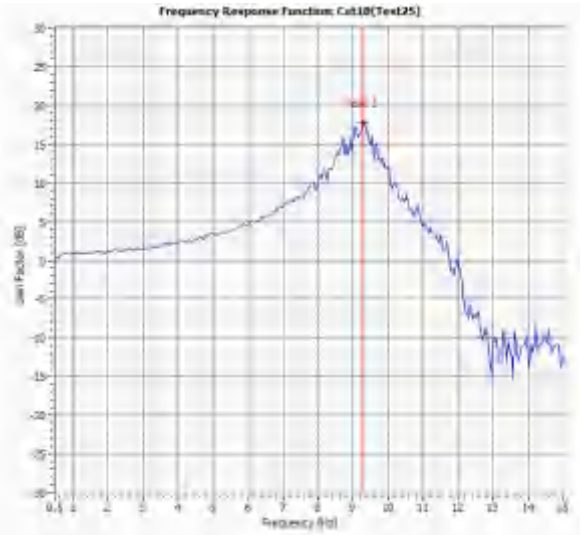

Fig. 9 - FRF peak picking for SPECIMEN III – cat10 (Test25)

During the experimental program all the channels identified in Figures 4 and 5 were recorded. As an example, Figures 10 and 11 show the results obtained for the NW top transverse acceleration and the NW top column displacement during the ElCentro 0.2g input, corresponding to Test2, Test5 and Test17. In these figures Plot 0 corresponds to the results obtained for SPECIMEN I, plot 1 for SPECIMEN II and plot 2 for SPECIMEN III.

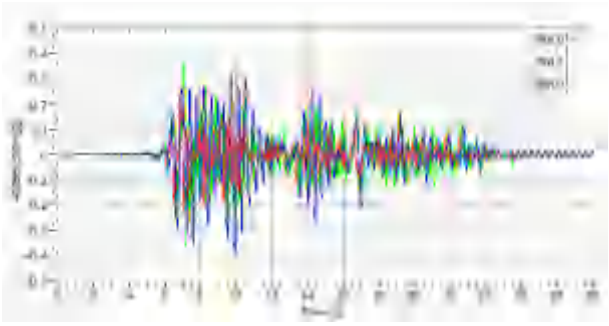

Fig. 10 – Comparison of NW top mass transverse acceleration

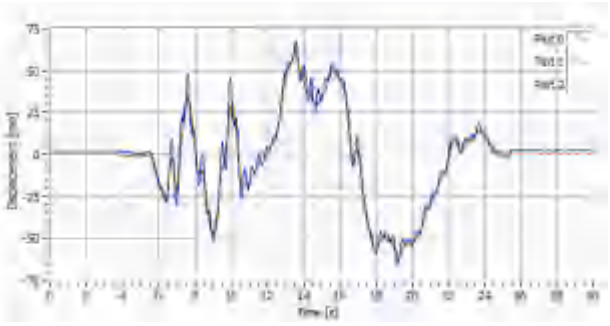

Fig. 11 – Comparison of NW top column transverse displacement

From the observation of these results it can be concluded that concerning accelerations, the SPECIMEN II was the one which has presented the lowest values at the top mass level. Concerning displacements, all the SPECIMENS have presented a similar behaviour.

Table 4 and 5 present the main results obtained for the specimens with dissipation devices. The maxima values recorded at the most representative channels are shown.

Table 4 - **Maxima values for the tests performed on SPECIMEN II (Frame with Dorka devices)**

	ElCentro 0.2g	EC8 0.2g	EC8 0.6g	EC8 0.8g	EC8 1g
NW top accel trans [g]	0.26	0.32	1.02	1.16	1.39
SW top accel trans [g]	0.27	0.37	1.11	1.25	1.51
Vert mass accel (CM) [g]	0.014	0.020	0.47	1.18	1.26
NW top column displ [mm]	63.34	26.23	78.92	104.40	110.20
SW top column displ [mm]	63.45	26.49	80.57	106.69	133.85
FNorth [kN]	10.49	14.47	42.87	49.43	56.98
FSouth [kN]	12.59	17.47	47.41	58.22	60.12
Displ North [mm]	0.27	0.40	1.03	1.75	4.02
Displ South [mm]	0.38	0.36	1.26	2.51	5.49

Table 5 - **Maxima values for the tests performed on SPECIMEN III (Frame with Jarrett devices)**

	ElCentro 0.2g	EC8 0.2g	EC8 0.6g	EC8 0.8g	EC8 1g
NW top accel trans [g]	0.37	0.27	0.89	1.50	1.70
SW top accel trans [g]	0.33	0.30	0.87	1.58	1.74
Vert mass accel (CM) [g]	0.007	0.009	0.05	0.09	0.13
NW top column displ [mm]	63.04	28.27	85.57	107.12	102.23
SW top column displ [mm]	63.35	28.65	86.30	114.06	133.63
FNorth [kN]	6.30	8.21	20.89	35.63	50.54
FSouth [kN]	6.76	8.63	21.63	39.48	54.81
Displ North [mm]	1.96	1.99	10.61	11.71	12.55
Displ South [mm]	1.95	1.89	10.33	12.00	12.48

In what concerns the top accelerations (NW and SW) the values obtained were similar for low and medium intensities while for the two highest levels bigger values for the Jarrett device were achieved. This can be explained by the specific characteristics of the materials used in this device (viscous fluid).

The clearly higher values of vertical mass acceleration obtained for the Dorka devices are due to the plastic behaviour of the steel cubes allowing vertical deformations for all levels of PGA intensity.

In spite of the different behaviour observed for the devices the values of maxima top displacements recorded at both columns were very similar due to the high rigidity of the common V bracing system adopted for both specimens.

Figures 12 and 13 present interaction diagrams of the force-displacement records at the North side Dorka dissipation device (SPECIMEN II), for a medium and the maximum EC8 input accelerations, respectively. Figures 14 and 15 present identical hysteretic loops for the North side Jarrett dissipation device (SPECIMEN III).

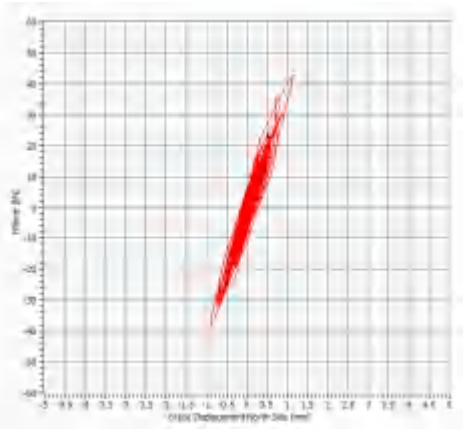

Fig. 12 – Hysteretic loops SPECIMEN II (EC8 0.6g)

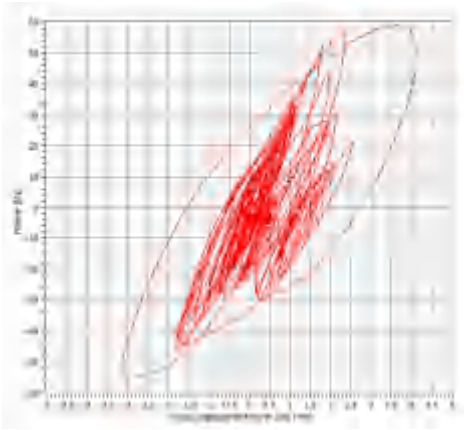

Fig. 13 – Hysteretic loops SPECIMEN II (EC8 1.0g)

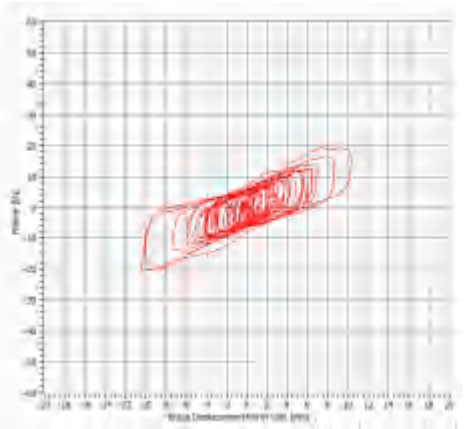

Fig. 14 – Hysteretic loops SPECIMEN III (EC8 0.6g)

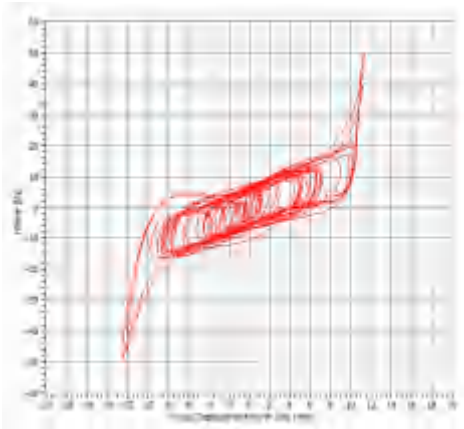

Fig. 15 – Hysteretic loops SPECIMEN III (EC8 1.0g)

From the observation of the previous figures it can be stated that apparently the Jarrett devices present a better dissipation performance with much higher displacements for the same levels of force when compared with the Dorka cubes.

It is also clear that the Jarrett characteristics are kept up to almost the maximum level of input accelerations achieved as it is presented in Figure 15 where it is shown that the changing of the global hysteretic loop shape appears only through final peaks in both directions.

Concerning the displacements recorded for both devices, for the Dorka the values have increased substantially from medium (0.6g) to high (1.0g) PGA values, while for the Jarrett those values were similar under both conditions. Although this fact, the Jarrett deformations were always extremely bigger thus proving their high capability. On the other hand when comparing the hysteretic loops for the Dorka devices from medium to high intensities there is a clear improvement due to the shear behaviour of the steel membrane used.

CONCLUSIONS

The experimental tests presented in this paper are part of a benchmark testing campaign that will analyse experimental results from two shaking table facilities (LNEC and NTUA) that have performed dynamic tests, a reaction wall laboratory (Ispra-JRC) that has performed pseudo-dynamic tests and a high-speed on-line sub-structuring installation (Univ. of Oxford).

All the tests were recently concluded and a global comparison of the results is under progress.

ACKNOWLEDGMENTS

The studies described in the present paper were financed by the European Union (contract HPRI-CT-2001-50023) under the NEFOREEE Project (New Fields of Research in Earthquake Engineering Experimentation) in the aim of the "Specific Research and Technological Development Programme" of the "Human Research Potential and Socio-Economic Knowledge Base". The cooperation of LNEC personnel, namely Eng. Campos Costa, Eng. Paulo Morais, Eng. Luis Mendes, Artur Santos, Ana Marques, Paulo Semedo and Dulcina Marecos, during the preparation and the performance of the shaking table tests, was deeply appreciated.

REFERENCES

[1] New Fields of Research in Earthquake Engineering Experimentation – University of Bristol technical report, U.K., 2001.
[2] Schmidt, K. and Dorka, U., Exp. Verification of Hyde-System, Paper 3163, 13thWCEE, Vancouver, Canada, 2004.
[3] Bairrao, R., Bursi, O., Carydis, P., Magonette, G., Mouzakis, H., Tirelli, D. and Williams, M., Benchmark Testing and Performance Comparison of Shaking Tables and Reaction Walls, 13th WCEE, Paper N. 441, Vancouver, Canada, 2004.
[4] Molina, F.J., Bairrao, R., Blakeborough, T., Bursi, O., Tirelli, D., Magonette, G., Mouzakis, H. and Williams, M.S., Testing performance benchmark for shaking tables and reaction walls within the NEFOREEE Project, 1stECEES, Paper 303, Geneva, Switzerland, 2006.
[5] SAP200NL, Structural Analysis Program, Computers and Structures Inc., Release 8.2.3, Berkeley, CA, 2003.
[6] prEN 1998-1, Eurocode 8: Design of structures for earthquake resistance. Part 1: General rules, seismic actions and rules for buildings, CEN, European Committee for Standardization, Brussels, Belgium, 2002.
[7] Bursi, O., Industrial application of shaking tables and reaction walls, NEFOREEE Project, University of Trento, 2004.